GeoStorage

Vol. 2, No. 2, p. 106-136, 2026

Research article

Leakage and Sealing in CO_2 Geological Storage: Driving Forces, Resistance and Mechanisms

Min Hao[1,2], Bing Bai[1]*, Haiqing Wu[1], Hongwu Lei[1], Hengtao Yang[1], Qixing Zhang[3,4], Lu Shi[1]

[1] *State Key Laboratory of Geomechanics and Geotechnical Engineering Safety, Institute of Rock and Soil Mechanics, Chinese Academy of Sciences, Wuhan 430071, China*
[2] *University of Chinese Academy of Sciences, Beijing 100049, China*
[3] *Hydro Geology and Engineering Geology and Environmental Geology Survey Institute of Qinghai Province, Xining 810008, China*
[4] *Hydrogeological and Geothermal Geological Key Laboratory of Qinghai Province, Xining 810008, China*

Keywords:
CO_2 geological storage
multi-scale characteristics
leakage modes
sealing definition
stress management

Cited as:
Hao M, Bai B, Wu HQ, et al. 2026. Leakage and Sealing in CO_2 Geological Storage: Driving Forces, Resistance and Mechanisms. *GeoStorage*, 2(2), 106-136. https://doi.org/10.46690/gs.2026.02.02

Abstract:
As a key strategy for achieving carbon neutrality, the safety and effectiveness of CO_2 geological storage depend on a thorough understanding of leakage dynamics and sealing mechanisms. Adopting a multi-scale perspective spanning pore, core, reservoir, site, and basin levels, this review systematically examines the structural characteristics of storage and migration spaces, identifies primary leakage pathways governed by faults, caprocks, and wellbores, and classifies dominant leakage modes. To address common conceptual ambiguities and scale disconnect issues in conventional studies, we propose a unified multi-scale definition framework based on the "object–process–boundary" concept, which clearly distinguishes among migration, transformation, sealing, and leakage behaviors. On this basis, we elucidate the dynamic coupling between driving mechanisms (e.g., buoyancy, pressure perturbation) and resistance mechanisms (e.g., capillary sealing, mineral reactions), and clarify their variations across scales and dimensions. Finally, a closed-loop "monitoring–prediction–regulation–intervention" framework, centered on stress management, is developed to provide systematic concepts and practical methodologies for risk assessment, monitoring design, and engineering control. This study provides a systematic synthesis across multiple scales, from pores to basins, forming a comprehensive foundation for assessing and ensuring the safety and efficiency of geological carbon storage projects.

1 Introduction

With the continuous increase in global energy demand and the intensification of climate change, carbon capture, utilization, and storage (CCUS) has become increasingly important for achieving carbon neutrality and has gradually progressed toward large-scale deployment (Bachu, 2008; Davis et al., 2018), being applied across diverse regions and multiple scales. By early 2025, the global operational CCUS capture and storage capacity had exceeded 50 million tons per year. Based on the current project pipeline, the capture capacity is projected to reach approximately 430 million tons per year by 2030, with a corresponding storage capacity of about 670 million tons per year (IEA, 2025). On the one hand, large-scale deployment highlights the core value of CCUS; on the other hand, it inevitably increases system complexity and potential risks. The risk of CO_2 leakage during storage remains a major obstacle to the widespread deployment of this technology.

CO_2 leakage is a critical issue for the safety of large-scale geological storage, and its prevention and control rely on well-sealed reservoir systems. The ideal reservoir is typically located at depths greater than 800 m (temperature >31.1 °C and pressure >72.8 bar), with sufficient pore space and high permeability to facilitate CO_2 injection and distribution, and is overlain by low-permeability caprock that prevents upward migration (Orr, 2009) (Fig. 1). Common storage media include deep saline

* Corresponding author.
E-mail address: 2951437199@qq.com (Hao M); bbai@whrsm.ac.cn (Bai B); Haiker1016@126.com (Wu HQ); hwlei@whrsm.ac.cn (Lei HW); htyang@mail.whrsm.ac.cn (Yang HT); zhangqixing114@163.com (Zhang QX); lshi@whrsm.ac.cn (Shi L)

Received Mar. 1, 2026; revised Mar. 10, 2025; accepted Mar. 15, 2026; available online Mar. 31, 2026.

Yandy Scientific Press

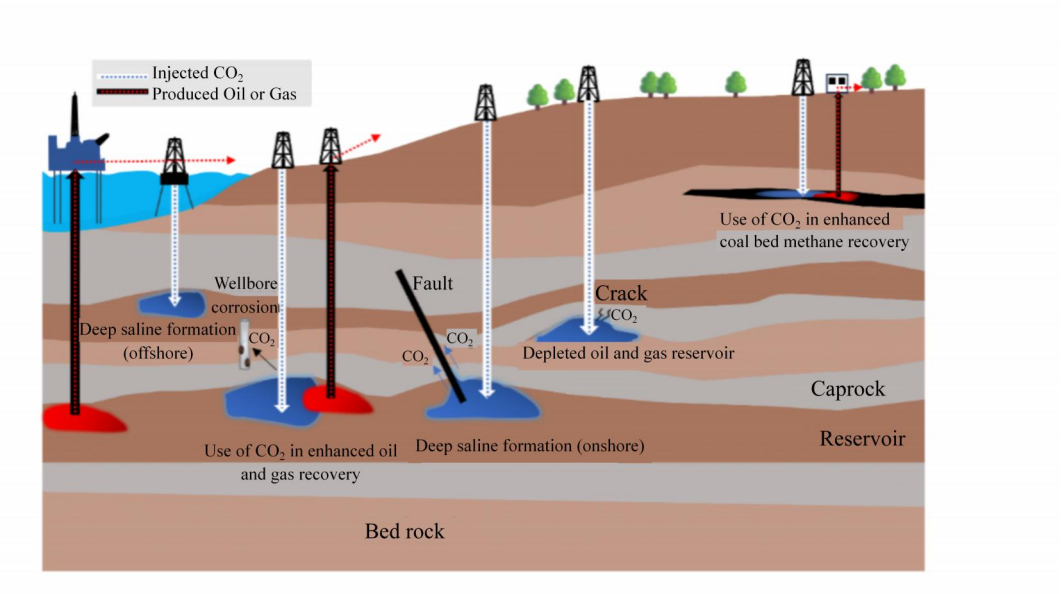

Fig. 1 Overview of geological storage options (modified after (Orr, 2009))

aquifers, depleted oil and gas reservoirs, salt or crystalline rock caverns, unminable coal seams, unconventional reservoirs, and igneous rocks (Jin et al., 2017; Raza et al., 2022; Sun et al., 2023; Davoodi et al., 2024). Through mechanisms such as structural and lithologic trapping, residual trapping, dissolution, mineralization, and coal-bed adsorption, these storage media enable CO_2 to remain for extended periods and effectively prevent escape (Dooley et al., 2006; Raza et al., 2016; Aminu et al., 2017).

However, there exists a dynamic interplay between sealing mechanisms and leakage pathways, which can essentially be attributed to a competitive process between driving and resistance forces. This mechanism operates across multiple scales (pores, cores, reservoirs, basins), and although specific parameters vary, they collectively determine the evolutionary outcomes of leakage and sealing (Luo et al., 2025). The process strongly depends on the multi-scale characteristics of storage and migration spaces and their dynamic evolution (De Silva et al., 2015; Yang et al., 2024). Among these, fault systems are particularly complex, as their discontinuities and associated fracture networks significantly increase the diversity and uncertainty of leakage pathways (Xu et al., 2022). Therefore, the long-term security of geological sequestration fundamentally depends on the precise definition and understanding of "leakage" and "sealing" behaviors. At present, there is still no unified and clear definition within academia and engineering for concepts such as "leakage" and related terms, including "migration", "transformation" and "sealing". Conceptual ambiguities not only hinder academic communication but also result in unreliable criteria for risk assessment and engineering design. Particularly in a multi-scale context, defining leakage behaviors across different levels—from pore and core to reservoir, site, and basin-has become a prerequisite for accurate modeling, monitoring, and management.

This review aims to systematically delineate the issues of leakage and sealing in CO_2 geological storage, beginning with fundamental concepts and focusing on the driving resistance force mechanisms and their multi-scale characteristics. The specific objectives are: (1) to reveal the multi-scale architecture spanning from pores to basins; to summarize the controlling effects and evolutionary patterns of the main potential leakage pathways (faults, caprocks, and wellbores) on CO_2 migration and sealing; and, based on this, to further propose a taxonomy of typical leakage modes categorized by pathway characteristics, leakage rate, and duration; (2) to propose a multi-scale definitional framework for leakage and sealing based on system boundaries, and to clarify the interaction mechanisms among driving forces, resistances, and pathways during leakage processes; and (3) to establish and synthesize a closed-loop framework centered on pressure management for "monitoring–prediction–regulation–intervention", thereby providing a systematic conceptual basis and an integrated analytical perspective for risk assessment and engineering control in CO_2 storage.

2 Multi-scale characteristics of storage - transport spaces and entities

The migration of CO_2 within subsurface reservoirs exhibits characteristic multi-scale behavior. The scope of study encompasses both geological entities (e.g., reservoirs and caprocks) and the CO_2 fluid under varying temperature and pressure conditions. At different scales, the flow mechanisms, sealing processes, and potential leakage risks of CO_2 exhibit distinct characteristics. Therefore, establishing a cross-scale conceptual framework is essential for understanding the overall storage and leakage behaviors of CO_2.

2.1 Multi-scale nature of storage systems and their components

Storage systems are inherently multi-scale, with their structural and behavioral characteristics varying significantly across scales. The scope of investigation extends across multiple

Tab. 1 Comparison of pore-scale numerical methods

Methods	Description	Applicability	Advantages	Disadvantages	References
Lattice Boltzmann Method (LBM)	Represents the fluid as a collection of particles and simulates multiphase flow through the interactions of particles in pore spaces.	Suitable for simulating the displacement behavior of CO_2-brine in porous media, taking into account factors such as wettability, viscosity ratio, and interfacial tension.	Simple to operate, computationally efficient, and capable of handling complex pore structures.	Limited applicability to CO_2-brine systems with realistic density and viscosity ratios in heterogeneous pore structures.	Liu et al., 2014; Jing and Tsuji, 2016; Fakhari et al., 2018; Guo et al., 2020; Sun et al., 2023
Pore Network (PN) Model	Simplifies pores into a lattice network of randomly shaped elements connected by throats, representing a simplified model of porous media.	Used to study CO_2 capillary trapping and the impact of mineral dissolution/precipitation on pore structure.	Computationally efficient, highly scalable, capable of simulating fluid flow in complex pore structures.	Ignores microscopic details, strongly parameter-dependent, lower accuracy, struggles to capture microscopic flow details.	Blunt et al., 2013; Bensinger and Beckingham, 2020; Campos et al., 2015; Benali et al., 2022; Liu et al., 2020
Smooth Particle Hydrodynamics (SPH)	A mesh-free method used to simulate the behavior of multiphase fluids at the pore scale.	Can be used for simulating CO_2 flow in porous media.	Relatively easy to implement.	Requires calibration of model parameters.	Hu et al., 2017
Computational Fluid Dynamics (CFD)	Simulates fluid flow based on the Navier-Stokes equations, effectively capturing interfaces.	Suitable for pore-scale multiphase flow simulation.	Capable of accurately capturing interface behavior.	Interfacial tension may cause numerical instability.	Ferrari et al., 2013
Phase-field LBM	A variant of LBM that describes multiphase flow based on phase-field theory.	Used to simulate multiphase flow characteristics in heterogeneous porous media.	Capable of handling complex interface behavior.	Numerical stability is limited for systems with high density/viscosity ratios.	Fakhari et al., 2018;
Shan-Chen LBM	Uses a pseudo-potential to describe interactions between different fluid phases.	Investigates relative permeability changes during CO_2-brine displacement processes.	Improved numerical stability and accuracy, particularly performing well under conditions of low resolution and low numerical viscosity.	Applicability to complex pore structures remains limited.	Shan et al., 1993; Sun et al., 2023

levels, from microscopic pores (μm–mm) and core fractures (cm–m) to fault zones (m–km) and regional basins (>km) (Fig. 2). Faults, as key structural elements within these systems, possess composite architectures typically composed of low-permeability fault gouge, high-permeability breccia, and surrounding fracture damage zones (Ducellier et al., 2011; Guglielmi et al., 2017). Research methodologies correspondingly vary with scale: laboratory studies typically use centimeter-scale core samples to simulate the seepage behavior of fault cores (Zhang et al., 2019a; Shen et al., 2021), whereas physical simulations and field tests are employed to investigate the controlling mechanisms of faults in realistic geological settings (Fernø et al., 2024; Michael et al., 2021).

The physicochemical properties of storage systems also exhibit pronounced multi-scale heterogeneity. Variations in mineral composition, stratigraphic architecture, fracture distribution, and pore morphology exert significant control on fluid migration and geochemical processes across scales—from pore to reservoir levels (Noiriel & Daval, 2017; Zhao et al., 2019).

The migration mechanisms of CO_2 likewise exhibit scale-

Tab. 2 Multiscale Processes, Controlling Factors, and Modeling Approaches in CO_2 Geological Storage

Scale	Spatial range	Dominant mechanisms	Key controlling factors/risks	Typical modeling approaches	Main applications
Pore scale (10 nm – 1 cm)	Pores, throats, micro-fractures	Capillary trapping, dissolution, mineralization, precipitation	Pore-throat size, geometry, roughness, wettability (contact angle), capillary entry pressure	Lattice Boltzmann (LBM), Pore-network (PN), CFD, SPH	Mechanistic understanding; constitutive parameters (e.g., permeability, relative permeability)
Core scale (1 cm – 10 cm)	Laboratory core samples, representative elementary volume (REV)	Multi-phase flow, fines migration, mineral dissolution/precipitation, capillary heterogeneity	Heterogeneity distribution, mineral reactivity, injection rate, wettability alteration, fines migration & clogging risk	CT-scanning, core-flooding experiments, pore-network upscaling, discrete element method (DEM)	Determination of REV, calibration of constitutive models, parameterization for reservoir-scale simulation
Reservoir scale (10 cm – 10^2 m)	Stratigraphic layers, lithological interfaces	CO_2–brine two-phase flow, viscous fingering, capillary barrier effect	Relative permeability, heterogeneity (lamination, mudstone interlayers), capillary pressure contrasts	H, HM, THM, THMC coupled models	Plume evolution, storage capacity, leakage assessment
Site scale (10^2 m – 10 km)	Traps, fault blocks, storage complexes	Plume migration, multi-well interference, fault reactivation	Geological structure, injection strategy, pressure build-up, stress perturbation	3D HMC coupled models; stochastic simulations	Risk evaluation, monitoring design, pressure management
Basin / regional scale (>10 km)	Sedimentary basins, clusters of storage sites	Source–sink matching, cumulative pressure effects, regional stress changes	Storage capacity, transport infrastructure, regional hydrodynamics, inter-site interference	System-level coupling models; techno-economic & policy scenario analysis	Regional deployment, strategic planning, policy support

dependent characteristics. The diffusion coefficient of CO_2 in porous media typically increases with the observation scale, with longitudinal dispersion capacity strengthening alongside scale and flow velocity gradients (Klotz et al., 1980; Appelo & Postma, 2004), whereas transverse dispersion remains relatively limited. At the field scale (km), the diffusion coefficient is generally 2–3 orders of magnitude higher than laboratory values and commonly increases with the measurement scale (Reimus & Callahan, 2007). Simultaneously, CO_2 migration in groundwater is strongly retarded by adsorption, leading to actual migration rates lower than average groundwater flow velocities (Dai et al., 2020). Adsorption behavior is highly sensitive to reservoir heterogeneity (Limousin et al., 2007), thereby increasing predictive uncertainties from the pore-throat scale to the field scale.

2.2 Multi-scale migration models and characteristics

Studies have shown that CO_2 migration exhibits distinct physical mechanisms and characteristics across different observational and characterization scales (Middleton et al. (2012)). The commonly adopted multi-scale models include the pore scale, core scale, reservoir scale, site scale, and basin or regional scale.

(1) Pore Scale (10 nm – 1 cm)

The pore system consists of diverse types, including intercrystalline pores, intergranular pores, dissolution pores (vugs), and fractures (Fig. 3), spanning scales from nanometers to centimeters (Al Haddad & Mancini, 2013; Gundogar et al., 2016). Nanopores constitute the primary spaces for CO_2 capillary trapping, whereas micron- to millimeter-scale dissolution pores and fractures form the dominant preferential flow pathways (Mitiku et al., 2013; Kang et al., 2015). At this scale, CO_2 migration is governed by multiple coupled physicochemical processes, including immiscible displacement, dissolution, capillary trapping, mineralization, and precipitation. The heterogeneity of pore structure (pore-throat diameter d , shape, roughness) and mineral surface wettability (contact angle θ) collectively determine the capillary entry pressure P_c, thereby controlling whether an individual pore-throat acts as a capillary barrier (Zhou et al., 2017; Ellis & Bazylak, 2012).

Pore-scale models typically allow a clear distinction between solid and pore phases, enabling accurate descriptions of coupled hydrodynamic and geochemical processes at solid–fluid interfaces. To elucidate pore-scale mechanisms, various numerical methods have recently been developed, including the lattice Boltzmann method (LBM), pore-network modeling (PNM), smoothed particle hydrodynamics (SPH), and computational fluid dynamics (CFD). Although CFD can accurately capture phase interfaces, it is often prone to numerical instabilities induced by surface tension. SPH is relatively straightforward to implement but requires parameter calibration. In contrast, LBM and PNM are widely adopted owing to their high efficiency and

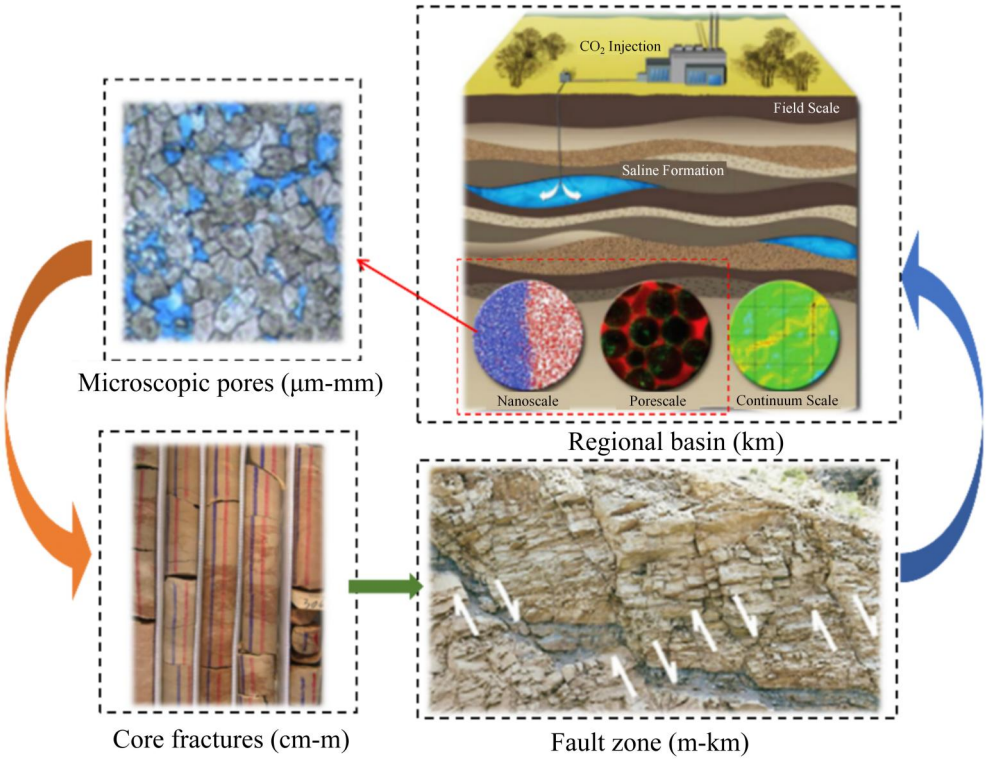

Fig. 2 Nanoscale to basin scale schematic diagram (modified after Evans and Bense (Evans, 2013; Bense et al., 2013))

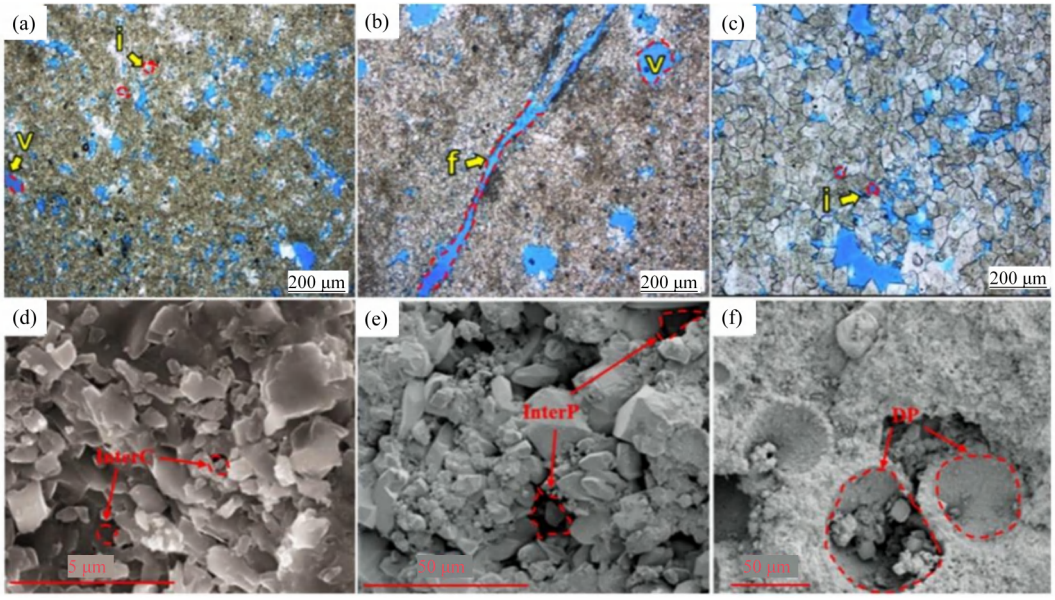

Fig. 3 Pore types in carbonate reservoirs: (a–c) Cast thin-section photomicrographs from northwest Iraq (Mohammed Sajed & Glover, 2020); (d–e) Scanning Electron Microscope (SEM) images from northern Iraq (Rashid et al., 2015). Labels: i and InterC: Intercrystalline pore; V: Vug; f: Fracture; InterP: Interparticle pore; DP: Dissolution pore (Tan et al., 2025)

broad applicability (Ferrari & Lunati, 2013; Hu et al., 2017) (Table 1).

A primary objective of studying CO_2 migration mechanisms and characteristics at the pore scale is to elucidate the emergent phenomena observed at macroscopic scales and to identify key controlling parameters, such as the capillary number—the ratio of viscous to capillary forces (Zhang et al., 2011). A second objective is to derive representative values of constitutive parameters, such as the permeability and relative permeability of porous media (Bachu & Bennion, 2008), thereby enabling more

realistic simulations at larger scales. Consequently, pore-scale modeling is essential not only for understanding the interactions among CO_2, reservoir rocks, and fluids but also for providing key parameters to calibrate reservoir-scale simulations (Sun et al., 2025). Furthermore, upscaling methods—such as volume averaging, homogenization theory, and fractal geometry—are applied to incorporate pore-scale processes into reservoir models (Zhang et al., 2021). However, the scale dependence of petrophysical parameters (e.g., permeability, diffusion coefficient) and reaction rates presents a major challenge for cross-scale prediction. For example, mineral dissolution rates at the field scale can be four to five orders of magnitude lower than those measured in the laboratory (White et al., 1996).

(2) Core Scale (1 cm – 10 cm)

The core scale serves as a critical bridge between pore-scale mechanisms and reservoir-scale behavior. Determining its Representative Elementary Volume (REV) requires comprehensive consideration of factors such as pore structure heterogeneity and multiphase fluid interactions. Experimental studies indicate that, following CO_2 injection, fine particles may migrate due to scouring at the CO_2–water interface, whereas residual water rings can immobilize some particles, collectively resulting in reduced permeability (Nguyen et al., 2024). Concurrently, mineral reactions exhibit marked lithological dependence: calcite-cemented sandstones may experience a pore volume increase of approximately 26.25%, whereas clay-cemented rocks show only about an 11.58% increase, underscoring the strong control of mineral reactivity on pore evolution (Wang et al., 2024). Furthermore, spatial heterogeneity in capillary forces can locally trap migrating CO_2, thereby enhancing lateral dispersion and reducing the risk of upward migration (Cui et al., 2024). Imbibition experiments further demonstrate that water flooding in CO_2-saturated cores can increase residual CO_2 saturation by 26–30%, primarily due to alterations in wettability and interfacial tension (Ge et al., 2022).

Migration patterns at the core scale are governed by the interaction between lithology and injection conditions. In calcite-cemented formations, pore enlargement and flow velocity can create a positive feedback loop, leading to unstable fingering phenomena. In contrast, clay-rich formations exhibit stable but constrained migration pathways due to strong capillary forces (Wang et al., 2025). Within nanopores of shale reservoirs, CO_2 displacement typically proceeds in three stages: pressure-driven flow, concurrent matrix–fracture production, and matrix release (Pan et al., 2025). CT imaging results reveal that pore heterogeneity strongly influences migration paths at low injection rates (0.1 cm^3/min), whereas this effect diminishes at higher injection rates (3 cm^3/min). This finding suggests that REV-scale parameters require dynamic adjustment during upscaling to account for specific injection conditions (Shi et al., 2010).

For upscaling, core-scale results can be transferred to the reservoir scale using methods such as pore-network modeling, volume averaging, and homogenization. For instance, pore-network models based on a truncated Weibull distribution indicate that miscible displacement efficiency is about 15% higher than that of immiscible displacement (Meng et al., 2014). At the same time, the effects of multi-field coupling must also be considered. Thermal–hydraulic–mechanical–chemical (THM-C) processes triggered by CO_2 injection may cause fault reactivation, necessitating reduced-order models for computational simplification (Li et al., 2025). In addition, discrete-element fluid–solid coupling models elucidate the microscopic mechanisms of particle migration and accumulation, with particle morphology and size distribution exerting a strong influence on parameterization outcomes (Yang et al., 2023).

(3) Reservoir Scale (10cm – 10^2 m)

Models at this scale are predominantly grounded in continuum mechanics principles, with the study domain typically extending from tens of centimeters to several hundred meters, depending on research objectives and computational resources. The primary focus lies in investigating the spatiotemporal evolution of the CO_2 plume within the reservoir. The resulting data are directly applicable to assessing reservoir capacity, injectivity, and potential leakage, and can also inform site-scale simulations. At this scale, capillary trapping plays a major role. Geological heterogeneities—such as cross-bedding, mudstone interlayers, and lithological interfaces—generate continuous zones of capillary pressure contrast. Even in the absence of absolute sealing layers, these heterogeneities can form "permeable traps," forcing buoyant CO_2 plumes to spread laterally and become immobilized beneath high-permeability units (Krevor et al., 2011; Krishnamurthy et al., 2022; Mishra & Haese, 2020)(Fig. 4).

Fig. 5. A conceptual sketch of the different scales of geologic heterogeneity and the CO_2 trapping mechanisms that can be observed at each scale. For example, capillary pinning is typically unobservable at microscopic scale, but it makes a systematic difference starting at the mesoscopic scale (Zhang et al., 2025).

Numerous studies have investigated this scale using a variety of multiphysics coupling models, including hydrological (H), hydrological–mechanical (H-M), thermal–hydrological–mechanical (THM), and thermal–hydrological–mechanical–chemical (THMC) models, among others (Fig. 5) (Bai et al., 2017; Cappa & Rutqvist, 2011; Carrillo & Bourg, 2021; Celia et al., 2015; Nordbotten et al., 2005; Rutqvist & Tsang, 2002; Rutqvist et al., 2007, 2008; Vilarrasa et al., 2011; Wu et al., 2016, 2018, 2021). The most fundamental characteristic of CO_2 migration at this scale is CO_2–water two-phase flow, which exhibits a spatiotemporal distribution characterized by viscous fingering. This phenomenon arises from the low density and viscosity of CO_2 relative to water (Nordbotten et al., 2005; Wu et al., 2016, 2018). Relative permeability is the most critical parameter governing this two-phase flow. At present, the relative permeability models most widely used in reservoir simulation software—primarily based on experimental data—are the Van Genuchten model and the generalized power-law model (Olivella et al., 1994; Rutqvist et al., 2002). In recent decades, pore-scale theoretical research has also led to the development of models that calculate relative permeability directly from interfacial tension, thereby establishing a direct link between pore-scale and reservoir-scale models (Bachu, 2008; Middleton et al., 2012).

(4) Site Scale (10^2 m – 10 km)

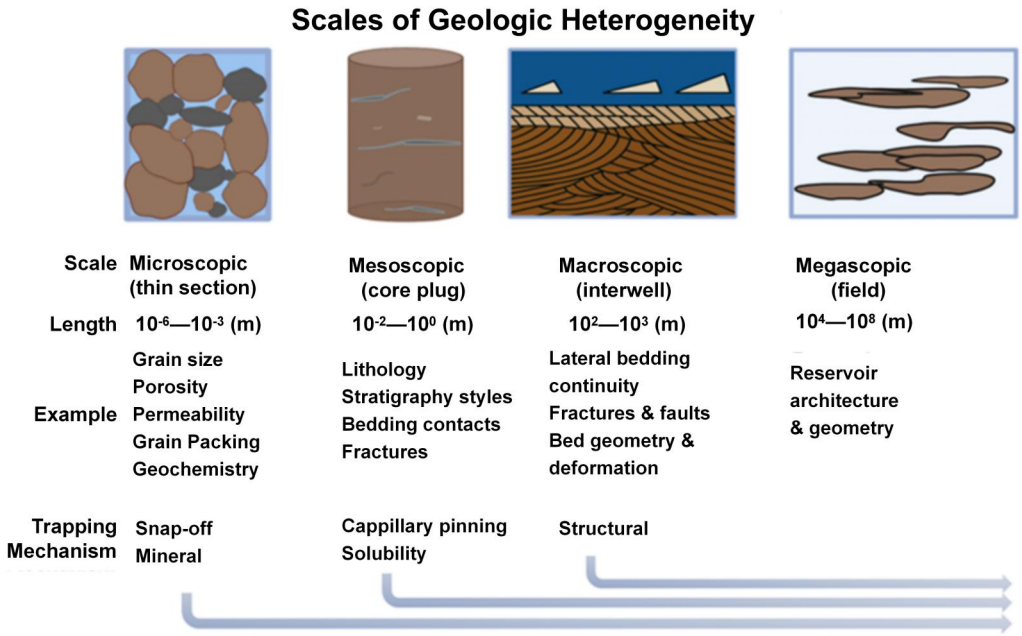

Fig. 4 A conceptual sketch of the different scales of geologic heterogeneity and the CO_2 trapping mechanisms that can be observed at each scale. For example, capillary pinning is typically unobservable at microscopic scale, but it makes a systematic difference starting at the mesoscopic scale (Zhang et al., 2025)

The site scale represents the core decision-making level that bridges reservoir characteristics with engineering practice. The study domain typically encompasses the entire storage complex (e.g., a complete anticlinal trap or fault block) and adjacent regions that may be affected. At this scale, factors such as formation dip and the spatial configuration of large-scale sedimentary units (e.g., bedsets) exert a strong influence. Dipping formations can divert vertically migrating CO_2 into long-distance lateral pathways, substantially increasing both the rock–fluid contact area and the residence time of CO_2 (Bryant et al., 2008; Ren et al., 2014). Models at this scale are designed to simulate and predict the spatiotemporal evolution of the entire CO_2 plume over decades of injection and centuries of post-injection monitoring, thereby supporting well placement optimization, risk management, and monitoring system design.

In addition to drilling engineering, pipeline layout, and groundwater systems, a central focus of site-scale analysis is the evaluation of synergistic and interference effects from multi-well injection. The simultaneous operation of multiple wells generates a superimposed pressure field that extends far beyond that of a single-well scenario. This elevated pressure field may activate far-field faults or induce microseismic events (Rutqvist, 2012). Consequently, site-scale simulations require highly refined 3D geological models and the integration of coupled processes—such as hydro-mechanical (HM) and thermo-hydro-mechanical-chemical (THMC) interactions—to assess the long-term integrity of the reservoir–caprock system under sustained injection (Celia et al., 2015).

Geological uncertainty constitutes the most critical challenge at this scale. To address it, stochastic modeling approaches (e.g., geostatistical simulation, Monte Carlo simulation) are frequently employed to generate multiple equiprobable geological realizations. These enable evaluation of confidence intervals for CO_2 migration pathways, storage efficiency, and leakage risk (Sun et al., 2023). Furthermore, inverse modeling techniques assimilate real-time monitoring data (e.g., pressure, temperature, geochemistry) from injection and observation wells to continuously update and calibrate models, thereby enabling dynamic optimization of predictions and establishing a closed-loop "simulate–monitor–update" management strategy (Li et al., 2023).

Ultimately, the outputs of site-scale research quantify leakage probabilities, define pressure management thresholds, optimize monitoring network configurations (e.g., well placement, seismic arrays, surface gas detection sites), and provide the scientific basis for safe injection protocols. This scale is thus pivotal for ensuring project safety and compliance within regulatory frameworks (Fig. 6).

(5) Basin/Regional Scale (>10 km)

Research at the basin scale bridges the transition from project-level safety management to regional energy system planning and climate policy formulation. This scale encompasses the entire system within a large sedimentary basin, including multiple storage sites, numerous CO_2 emission sources, and the associated transportation infrastructure (e.g., pipeline networks) that connects them. The core objectives are source–sink matching optimization and system-level risk management. On the one hand, this involves assessing the basin's total storage capacity and, by comprehensively considering reservoir properties, capacity, costs, and source–sink distances, planning

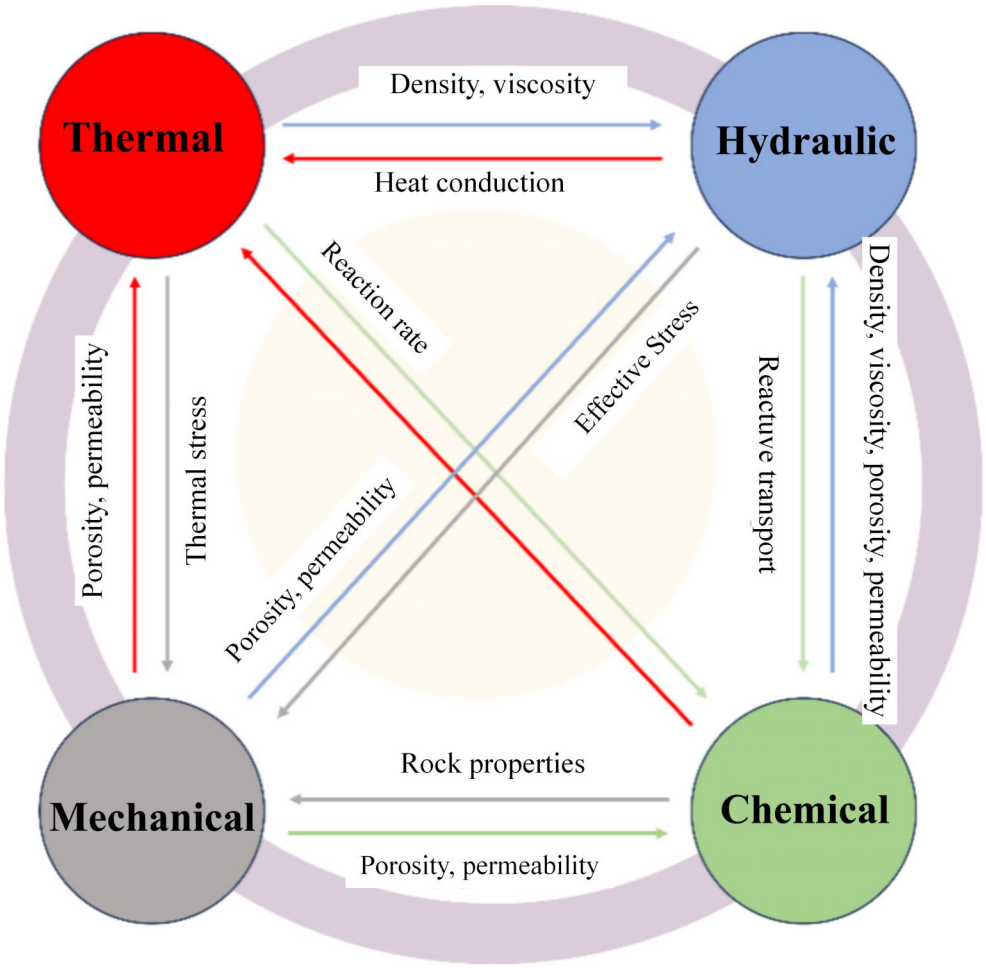

Fig. 5 THMC coupling of CO_2 geological storage (modified after (Sun et al., 2025)

optimal pipeline routing and storage deployment sequences to maximize the cost-effectiveness of CCUS clusters (GCCSI, 2023). On the other hand, the simultaneous large-scale development of multiple sites may produce cumulative regional effects. Injection operations at one site can elevate pore pressure, with the resulting pressure front propagating over tens of kilometers. Such effects may inadvertently influence neighboring storage sites or subsurface resources (e.g., geothermal reservoirs, freshwater aquifers) and could even induce regional modifications to the in-situ stress field (Birkholzer et al., 2009). Accordingly, basin-scale investigations commonly employ multi-site coupled models or system assessment frameworks that simplify detailed fluid-flow processes. These models must integrate economic cost functions, policy incentive schemes, infrastructure planning modules, and simplified porous media flow representations to conduct long-term (decadal to centennial) scenario analyses and sensitivity assessments. CO_2 storage and transport processes inherently span multiple scales—from pore and reservoir to site and basin—each dominated by distinct mechanisms, controlling parameters, and key risk factors (Tab. 2). The pore scale governs interfacial interactions and trapping mechanisms; the core scale, through experiments and detailed simulations, reveals the averaged effects and macroscopic expression of pore networks; the reservoir scale elucidates plume dynamics; the site scale emphasizes pressure-field coupling and monitoring requirements; and the basin scale addresses regional deployment and strategic security. Multiscale coupling is thus not only a fundamental scientific challenge but also a prerequisite for establishing a robust framework for leakage assessment and sealing evaluation.

3 Carbon Storage Systems and Potential Leakage Pathways & Modes

3.1 System Components and Leakage Pathways: An Overview

An ideal carbon storage system consists of a reservoir and an overlying caprock. The sealing capacity of the system determines the ultimate fate of CO_2, whereas inherent geological heterogeneities and engineering interventions govern the formation of potential leakage pathways. Essentially, leakage is not an independent process separate from storage but a specific manifestation of CO_2 migration. Within a typical reservoir, CO_2 migration is governed by the interplay between driving and resisting forces. When the resisting forces are insufficient to counteract the driving forces, CO_2 can breach sealing barriers, resulting in leakage events across multiple scales.

Common potential leakage pathways comprise engineered pathways (e.g., poorly sealed or abandoned wellbores), natural

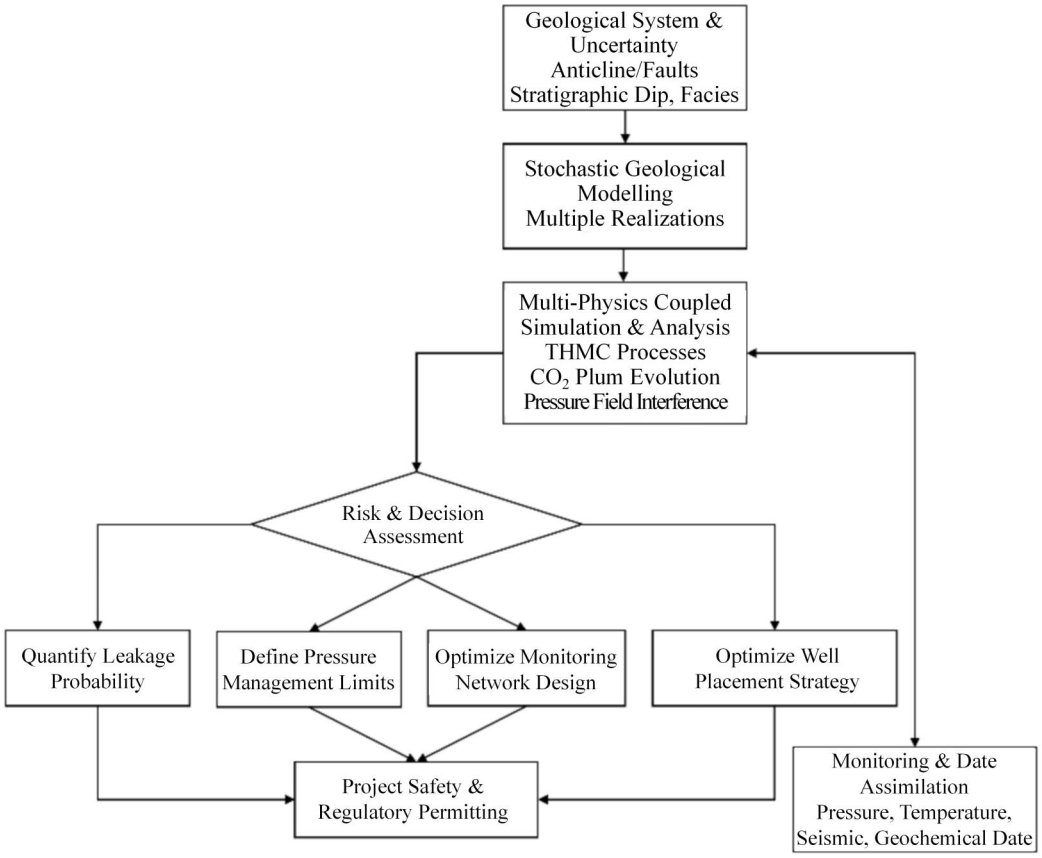

Fig. 6 The core logic of site scale research

pathways (e.g., faults, fractures, localized high-permeability zones), and hybrid pathways. According to the RISCS project, CO_2 leakage modes are classified into three types:

(1) localized point-source leakage (e.g., from wells experiencing seal failure),

(2) localized multi-point leakage distributed linearly along faults or fractures,

(3) diffuse, large-area leakage (commonly occurring in sediments or soils) (Pearce et al., 2014) (Fig. 7). Among these, the first two types are most prevalent, as CO_2 preferentially migrates along high-permeability pathways. Diffuse leakage is generally less likely; however, if it occurs, it poses a risk at a regional scale. Consequently, the primary potential leakage pathways in carbon storage systems are mainly associated with faults, the caprock, and wellbores (Adamu et al., 2019; Chen et al., 2024a).

3.2 Potential Leakage Pathways and Modes

3.2.1 Leakage Mechanisms and Dynamic Behavior of Faults

Faults constitute one of the most critical potential leakage pathways in geological storage systems. Their permeability characteristics directly influence storage security and are governed by the combined effects of multiple factors, including fault zone architecture, lithology, and in-situ stress conditions. A typical fault zone comprises a low-permeability fault core (gouge), a high-permeability damage zone (breccia and fractures), and a peripheral fracture damage zone, collectively forming a structurally complex migration conduit (Ducellier et al., 2011)(Fig. 8). Fault reactivation can potentially induce seismic events and simultaneously create pathways for the leakage of CO_2 and brine, thereby threatening the safety of nearby potable aquifers. During their evolution, faults exhibit diverse structural configurations, ranging from a single slip surface or sealed pores to complex permeable networks comprising a fault core and damage zone; their geometric characteristics determine their capacity and behavior as potential leakage conduits (Sun et al., 2025). Numerical simulations suggest that the heterogeneous distribution of faults may act as a "double-edged sword": while it can disperse CO_2 into multiple caprock regions, enhancing storage efficiency, it may also, if faults extend through the caprock, directly result in leakage (Zhang et al., 2024b).

The kinematic behavior of faults, particularly shear slip, dynamically modifies leakage pathways. Fault activation and slip can significantly alter their internal architecture (e.g., generating fault gouge, creating new fractures), resulting in substantial changes in permeability (Zhu et al., 2020; Shen et al., 2021). Injection-induced increases in pore pressure effectively reduce the normal stress acting on the fault plane, thereby triggering fault slip according to the slip criterion. This coupled process, known as hydro-mechanical coupling, represents a key kinematic mechanism controlling the potential of a fault to act as a leakage conduit (Guglielmi et al., 2021).

The mechanical and hydraulic behavior of faults is typically

Tab. 3 Summary of Caprock Integrity Research.

Aspect	Key Findings & Conclusions	Corresponding References
Geometrical Features	1. Caprock Thickness: A key physical barrier against vertical fracture penetration. Plastic strain can propagate through the entire thickness. 2. Fracture/Fault Geometry: Includes orientation, dip, frequency, and spatial distribution. These features, controlled by in-situ stress fields and fluid pressures, are potential leakage pathways. 3. Interface Geometry: The boundary between the caprock and reservoir (e.g., caprock-aquifer interface) is a zone of stress and strain concentration, prone to failure. 4. Reservoir Geometry: The lateral extent and depth of the reservoir influence the extent of pressure propagation and buildup, thereby affecting the stress imposed on the caprock.	Peacock and Mann, 2005; Raziperchikolaee and Pasumarti, 2020
Sealing Mechanism	The caprock should be dense, intact, and have low permeability to maintain a supercritical CO_2 state and prevent leakage.	Watson and Gibson-Poole, 2005; Shukla et al., 2010
Failure Modes	1. Fracture Formation & Reactivation: Pore pressure changes from injection can alter effective stress, potentially initiating new fractures or reactivating existing faults. 2. Plastic Strain Propagation: Plastic strain can spread through the caprock's thickness when vertical stress exceeds horizontal stress, facilitating CO_2 migration. 3. Capillary Barrier Breakdown: High-stress conditions can potentially breach the caprock's capillary barrier. 4. Chemical Degradation: High-salinity fluids can lead to mineral evaporation and crystallization (e.g., carnallite, halite), reducing pore connectivity.	Song and Zhang , 2013; Vilarrasa et al., 2011; Orlic et al., 2011; Jayasekara et al., 2020
Influencing Factors	- Stress State: Initial stress state, ratio of horizontal to vertical stress. - Injection Pressure & Temperature: High-pressure injection may exceed fracture pressure; cold CO_2 injection can promote horizontal fracture propagation. - Fluid Properties: Salinity, CO_2 saturation, capillary entry pressure. - Rock Properties: Young's modulus, permeability, porosity, hysteresis coefficient. - Geological Structure: Fault orientation, fracture distribution, bedding heterogeneity.	Raziperchikolaee and Pasumarti, 2020; Martinez et al., 2013; Pan et al., 2013; Raziperchikolaee et al., 2019; Khan et al., 2024
Research Methods	- Numerical Simulation (coupled flow-geomechanical models) - Experimental Studies (triaxial tests, breakthrough pressure tests) - Probabilistic Modeling (Monte Carlo simulation, response surface methodology) - Field Monitoring (microseismic, pressure monitoring) - Imaging Techniques (3D Digital Image Correlation - 3D-DIC)	Rutqvist, 2012; Raziperchikolaee et al., 2013b; Adisornsupawat et al., 2024; Lee et al., 2023; Nath et al., 2024
Protection/ Mitigation Measures	- Control injection pressure to avoid exceeding fracture pressure. - Prefer high-salinity formations to enhance caprock sealing. - Use nanoparticles or surfactants to improve caprock wettability and enhance sealing capacity. - Implement monitoring and early warning systems (pressure, microseismic, geochemical monitoring). - Conduct integrity assessments and re-plug wells (reopen and re-plug high-risk wells).	Bai et al., 2015; Jayasekara et al., 2020; Khan et al., 2024; Yang et al., 2019

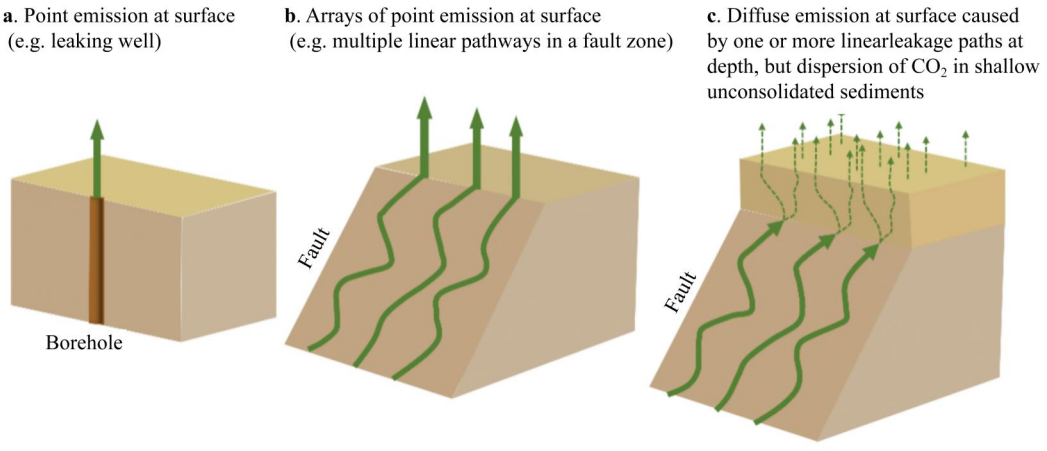

Fig. 7 Three types of CO_2 leakage modes classified by the RISCS project (Pearce, J. et al., 2014)

Tab. 4 Potential Leakage Paths, Mechanisms, and Kinetic Behavior in CO_2 Geological Sequestration.

Aspect	Fault	Caprock	Wellbore	Multiphysics-Chemical Coupling
Leakage Pathway	Fault	Caprock	Wellbore	Multiphysics-Chemical Coupling
Structure/Composition Characteristics	Fault gouge (low permeability), fractured rock (high permeability), fracture damage zone	Mudstone, evaporites, carbonate rocks	Casing–cement–formation interfaces; artificial construction defects	Pore–mineral–fluid interface reactions; micro-to-reservoir scale effects
Controlling Factors	Geometric characteristics, heterogeneity, stress field, pore pressure disturbance	Pore pressure, fracture orientation and stress field alignment, heterogeneity	Cement quality, material properties, temperature-pressure cycling, construction defects	Temperature-pressure conditions, salinity, mineral composition
Main Leakage Mechanisms	Shear slip modification, permeability change; fault reactivation; channeling effect	Hydraulic fracturing; shear-induced rupture; dissolution expansion; overpressure	Interface debonding; cement cracking; casing corrosion; screw thread leakage	CO_2 dissolution–acid–mineral reaction/precipitation; permeability evolution coupled with porosity
Mechanical Behavior	Shear stress increase → fault slip; injection pore pressure increase → effective stress decrease; fault structure rearrangement	Injection rate and stress state controlled fracture propagation; vertical stress dominates normal fracture opening; horizontal stress dominates oblique shear	Injection–sealing period affected by stress distribution; thermal–chemical–mechanical coupling leads to weak sealing; micro-leakage aggravation	Cumulative micro-reaction → permeability nonlinear evolution; mineral reaction alters mechanical strength; THMC coupling → flow field restructuring
Typical Mode	Layer-permeated leakage vs. dispersed injection	Hydraulic fracture; shear failure leakage	Annular flow; cement channel leakage	Pore-scale reaction → reservoir weakening → leakage channel formation
Research Methods	Core experiments, physical modeling, numerical modeling, discrete element/finite element modeling, Mohr-Coulomb criterion	Fracture pressure tests, caprock mechanics experiments, numerical modeling (THM coupling)	Engineering diagnosis, monitoring, finite element simulation (FEM, THM coupling)	Reactive transport modeling (pore scale/continuum), cross-scale modeling (THMC coupling)

Tab. 5 Unified definitions of migration, leakage, and sealing across multiple scales.

Scale	Migration	Leakage	Sealing	Measurable Sealing Metric
Pore scale ($m--mm$)	CO_2 movement or phase transformation within pores and throats	Breakthrough of pore throat into adjacent fractures or matrix	Capillary trapping, residual trapping, mineral transformation	Capillary Entry Pressure (P_{ce}), Residual CO_2 Saturation (S_{gr}), Contact angle (θ).
Core/fracture scale ($cm--m$)	CO_2 migration within core samples or fracture networks	Penetration through fractures or damage zones	Fracture self-sealing, pore clogging, mineral precipitation	Breakthrough Pressure (P_b), Relative permeability hysteresis, Fracture transmissivity reduction rate.
Reservoir scale ($m--km$)	CO_2 migration and accumulation beneath caprock within the reservoir	Breakthrough of caprock or upward migration along faults	Structural/lithologic trapping, caprock sealing, dissolution trapping	Maximum Sealing Pressure, Fault reactivation pressure, Seal Capacity.
Site scale ($km--10km$)	CO_2 redistribution within storage site	Exceeding monitoring boundary or entering shallow aquifers	Pressure management, monitoring and control	Area of Review extent, Pressure interference threshold between wells.
Basin scale ($10--100km$)	Regional redistribution of CO_2	CO_2 migration into shallow aquifers, atmosphere, or ecosystems	Regional sealing, structural traps, multi-site integrated management	Integrated basin-scale risk metric (e.g., Probability of Release$< 10^{-6}yr^{-1}$).

Tab. 6 Multi-scale and Dimensional Characteristics of Resistance and Driving Force Attenuation Effects in Geological CO_2 Storage.

Scale Level	Pore-Core Scale	Reservoir-Fault-Seal Scale	Regional-Basin Scale
Spatial Range	*m – cm*	m - km	km - 100+ km
Dominant Driving Forces	Buoyancy, Pressure gradient	Buoyancy, Pressure gradient, Flow induced by heterogeneity	Regional pressure regime, Basinal thermo-fluid field
Dominant Resistance Mechanisms	Capillary trapping, Mineral dissolution/precipitation	Fault/fracture sealing, Lithological heterogeneity, Seal breakthrough pressure	Macroscopic structural trapping (anticlines, synclines), Regional seal integrity
Effect Characteristics & Attenuation Laws	Strong attenuation. Resistance mechanisms significantly inhibit CO_2 migration at early stages, manifesting as residual trapping and permeability alteration.	Duality and abruptness. Resistance efficacy depends on structural sealing but can be rapidly overcome by highly connected fracture networks, leading to "conduit-flow" leakage.	Non-linearity and catastrophic potential. Resistance provides the ultimate sealing constraint. A critical pressure breach leads to large-scale, sudden release. Driving force attenuation is highly non-linear.
Dimensional Effects & Modeling Insights	Pore-network models (3D). Neglecting 3D pore structure overestimates permeability and migration rates.	3D simulation is crucial. 2D models severely underestimate lateral dispersion and leakage risk along faults. Fracture flow approximates 1D pipeline flow, drastically accelerating leakage.	3D geomechanical models. 2D models fail to capture the volume of complex traps and the overall stability of the seal. Upscaling is key for accurate prediction.

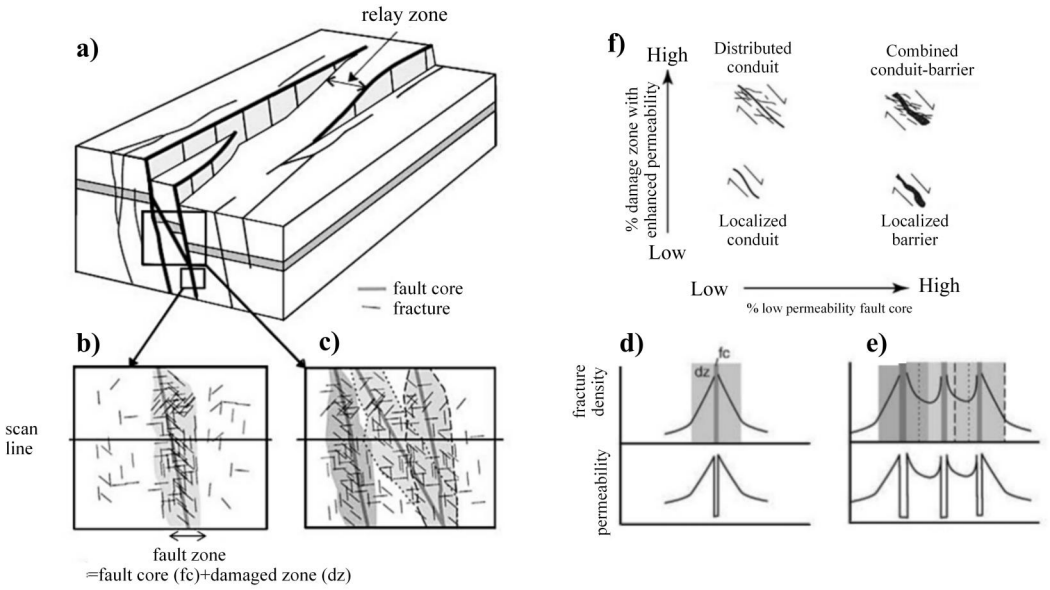

Fig. 8 (a) 3D block diagram showing a normal fault zone (Childs et al., 2009). (b, c) Definitions of fault zone width for single-strand and multi-strand faults, respectively (Chester & Logan, 1986; Caine et al., 1996; Faulkner, 2004; Faulkner et al., 2010). (d, e) Conceptual fracture density and permeability profiles for crystalline bedrock in single and multi-strand fault zones (modified after (Faulkner et al., 2010; Bense et al., 2013)). (f) Fault classification based on the proportion of fault core to damage zone (Caine et al., 1996)

characterized using numerical modeling, which generally falls into two categories. The first approach employs continuum elements, enabling the assignment of various constitutive models (e.g., elastic, elasto-plastic, or visco-plastic) to the fault zone. This approach can represent internal heterogeneity within the fault zone and its interaction with the surrounding rock mass; however, it becomes computationally expensive when modeling large slip displacements and complex geometries (Cappa & Rutqvist, 2011; Morris et al., 2011). The second approach utilizes interface elements, treating the fault as a discrete surface characterized by parameters including friction, cohesion, and stiffness. This approach is well-suited for simulating fault reactivation across multiple scales and within complex fault networks (Li et al., 2006; Cappa & Rutqvist, 2011). Fault re-

activation generally follows the Mohr-Coulomb criterion (Fig. 9) and may occur when the shear stress acting on the fault plane exceeds the Mohr-Coulomb failure threshold (Jaeger et al., 2009), expressed as:

$$|\tau_s| \geq c + \sigma_n tan\phi \quad (1)$$

Where τ_s is the shear stress, σ_n is the normal stress, c is the cohesion, and ϕ is the friction angle. The primary controlling parameters are the friction coefficient and cohesion. This framework can be extended through slip-weakening models or rate-and-state friction laws to distinguish between seismic and aseismic slip processes. These modeling frameworks not only elucidate the underlying mechanisms of fault kinematic behavior but also offer critical support for assessing leakage risks during CO_2 storage operations.

3.2.2 Caprock Integrity and Failure Modes

The caprock, acting as the primary barrier overlying the reservoir, relies on its low permeability and significant mechanical strength to prevent upward migration. Key sealing mechanisms of the caprock include capillary sealing, hydraulic sealing, overpressure sealing, and hydrocarbon concentration sealing (Rutqvist, 2012; Shukla et al., 2010). The effectiveness of a carbon storage system depends on the integrity of the caprock. However, in realistic geological settings, caprocks are rarely perfectly homogeneous and may contain fractures, weak planes, or heterogeneous zones, which serve as potential leakage pathways. Typical caprocks comprise argillaceous rocks (shale, claystone, mudstone), evaporites (salt, anhydrite), and, in certain cases, carbonate rocks (limestone, dolomite) (Griffith et al., 2011). These lithologies exhibit notable differences in fracture development, pore structure, and weak plane distribution; their geometric characteristics govern potential CO_2 migration modes

CO_2 leakage through the caprock may occur via multiple mechanisms, including hydraulic fracturing, induced shear failure, leakage along pre-existing faults, dissolved gas diffusion, pore pressure exceeding the breakthrough pressure, or leakage through wellbores. The primary geomechanical failure modes include hydraulic fracturing and induced shear failure (Fig. 10). Hydraulic fracturing is triggered by excessive injection pressure; however, this risk can be largely mitigated by maintaining injection pressure below 90% of the fracturing pressure (Lecampion et al., 2018; Chen et al., 2021). Induced shear failure occurs when the shear stress exceeds the shear strength, typically evaluated using the Mohr-Coulomb failure criterion (Zhang et al., 2015), analogous to fault reactivation. Key factors affecting caprock integrity include the orientation of fractures relative to the in-situ stress field, the magnitude of the minimum horizontal stress, injection rate, and the initial stress state (Peacock & Mann, 2005; Karimnezhad et al., 2014; Raziperchikolaee & Pasumarti, 2020).

Rutqvist et al. reported that shear failure generally occurs at lower injection pressures than hydraulic fracturing (Rutqvist et al., 2008). When horizontal stress exceeds vertical stress, shear failure preferentially occurs along low-angle fractures, which may not compromise the upper portions of the caprock. However, when vertical stress exceeds horizontal stress, fracture propagation is more likely to occur as steeply dipping fractures that may penetrate the entire caprock sequence. Numerical modeling indicates that the lower portion of the caprock is more susceptible to pore pressure changes, whereas the overall caprock generally remains stable under appropriate operational conditions (Rutqvist & Tsang, 2002; Sun et al., 2023).

Caprock breakthrough pressure represents the most direct and critical parameter for assessing its sealing capacity. If CO_2 pressure exceeds this threshold, preferential flow pathways may form within the caprock, potentially allowing CO_2 leakage. Moreover, CO_2 adsorption can reduce shale permeability but may also induce pressure buildup and decrease frictional strength (Birkholzer et al., 2009; Song & Zhang, 2013). Thermo-chemical-mechanical (TCM) coupling effects can generate local negative effective stresses and promote mineral precipitation, thereby modifying caprock sealing performance (Xiao et al., 2020; Thompson et al., 2021). Consequently, although the overall caprock typically maintains good sealing capacity, local instabilities and reactivation can still generate potential pathways for CO_2 leakage.

3.2.3 Wellbore Leakage: An Engineering Vulnerability

Wellbores, acting as the primary conduits connecting the surface to the subsurface, contain interfaces (casing-cement, cement-formation) that constitute potential weak points (Fig. 11). Wellbore integrity—defined as the capacity to maintain sealing and isolation functions during CO_2 storage—represents a critical factor for ensuring safe sealing. Compared with geological features (e.g., faults, fractures), wellbores are more susceptible to acting as potential leakage pathways due to their engineered nature (Bachu & Watson, 2009; Wigand et al., 2009). This aspect of integrity relates to the ability to maintain zonal isolation throughout the storage lifecycle, primarily encompassing internal mechanical integrity (sealing of tubing, casing, packers, etc.) and external integrity (sealing of the casing-cement-formation system).

Existing studies indicate that wellbore failure can result from multiple factors, including chemical reactions (e.g., cement carbonation, Eq. (2)), thermo-mechanical loading, or construction defects, potentially leading to the formation of multiple leakage pathways. Typical leakage conduits include casing corrosion, incomplete cement placement, flow through micro-annuli or open-hole sections, casing thread leaks, interfacial debonding, poor cement consolidation, and fractures or channels within the cement sheath (Reinicke & Fichter, 2010; Carroll et al., 2016).

$$\begin{aligned} &CO_{2(aq)} + H_2O \rightarrow HCO_3^- + H^+ \\ &Ca(OH)_{2(s)} \rightarrow Ca^{2+} + 2OH^- \\ &Ca^{2+} + HCO_3^- + OH^- \rightarrow CaCO_{3(s)} + H_2O \\ &H^+ + CSH_{(s)} \rightarrow Ca^{2+} + H_2O + SiO_2 \cdot H_2O_{(s)} \end{aligned} \quad (2)$$

During drilling, casing, cementing, hardening, and injection operations, the wellbore and surrounding formation undergo stress redistribution and changes in material properties: drilling modifies the in-situ stress distribution; cement shrinkage during hardening may cause interfacial debonding; and temperature

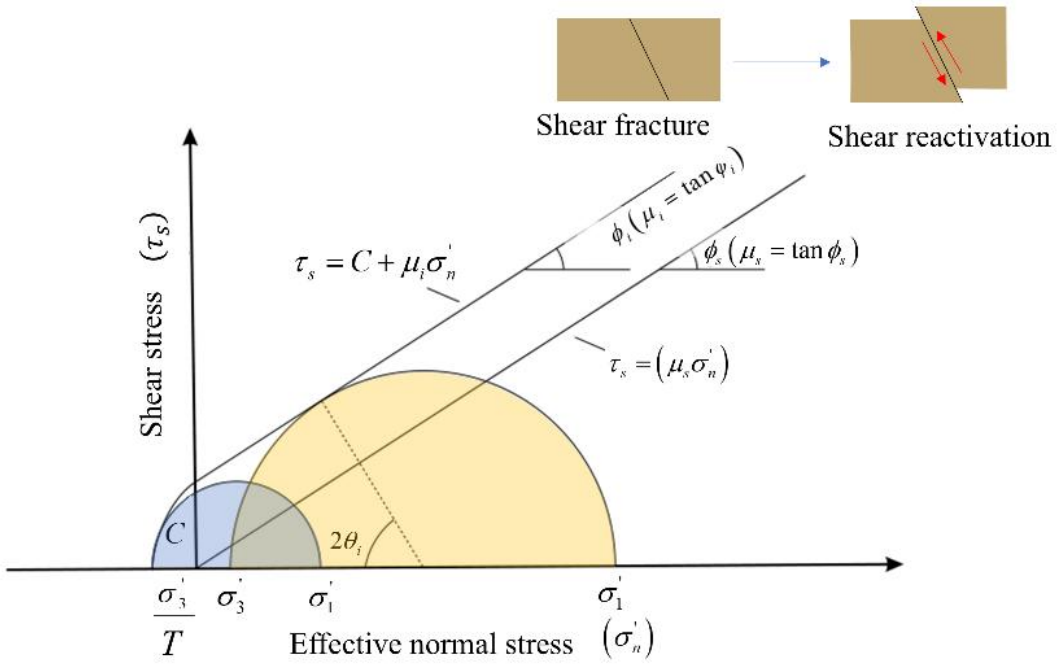

Fig. 9 Schematic diagram of shear fracture and reactivation mechanism based on Mohr-Coulomb criterion (modified after Mildren et al., 2005)

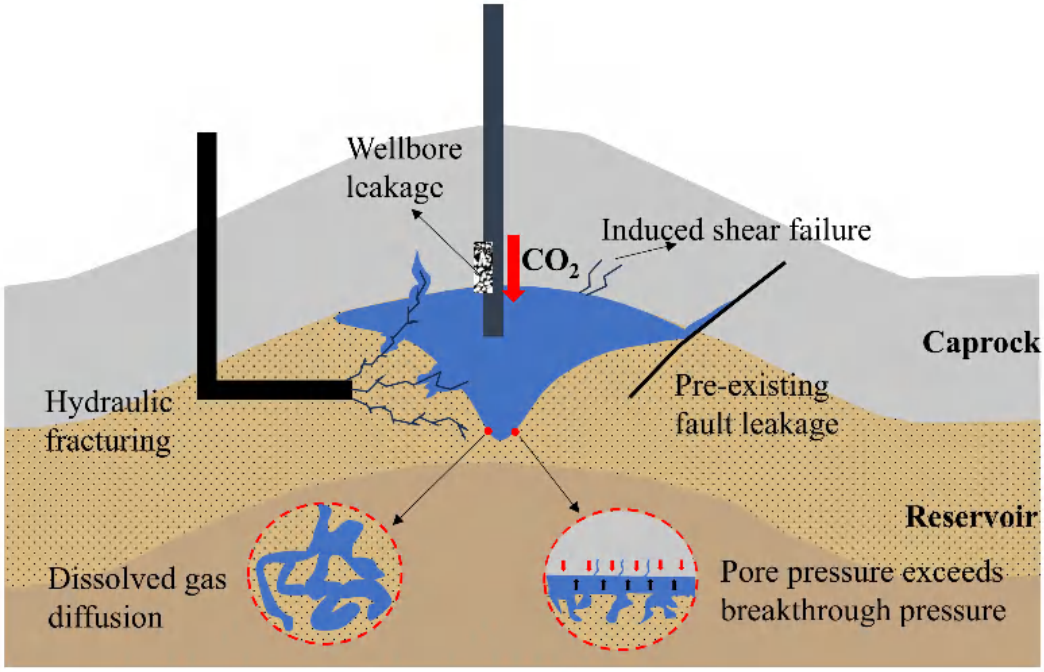

Fig. 10 The schematic diagram of the CO_2 leakage paths of the cap rock

differences induced by CO_2 injection generate thermal stresses, further promoting fracture formation or interface failure (Gray et al., 2009; Zhang, 2013; Nygaard et al., 2014). Simultaneously, increasing pore pressure can degrade cement integrity and may trigger caprock fracturing or the reopening of existing fractures. Moreover, acidic fluids and CO_2-saturated formation water can corrode casing and cement, thereby reducing bond strength and sealing capacity. During the migration and long-term storage phases, injection wells, abandoned wells, and unidentified faults or fractures may evolve into leakage points. Stress field changes induced by increasing pore pressure may also trigger microseismic events, further exacerbating integrity degradation in the wellbore and adjacent caprock. To address these risks, geomechanical numerical modeling has emerged as

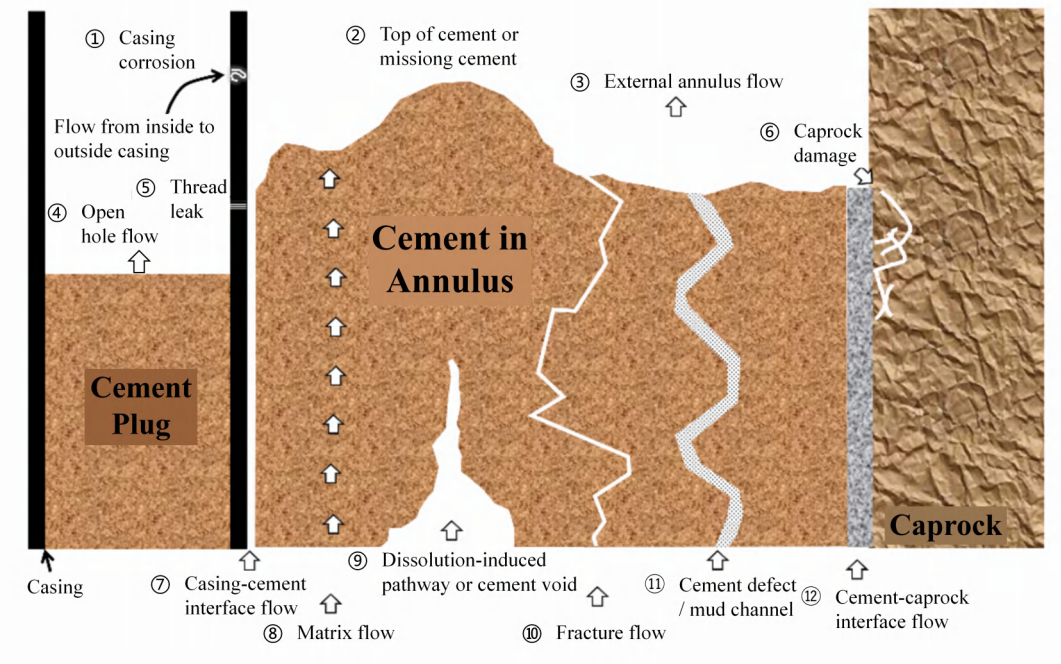

Fig. 11 Potential leak pathways through an abandoned well (modified after (Carroll et al., 2016))

a critical tool for predicting the stress-deformation response and potential failure modes of the wellbore and adjacent formations throughout the injection and storage lifecycle (Li et al., 2023; Sun et al., 2024). The Finite Element Method (FEM), renowned for its capability to handle complex geometries and material nonlinearity, is extensively employed in wellbore integrity analysis, often integrated with coupled thermal-hydrological-mechanical (THM) processes. For example, simulations for the Northern Lights CCUS project in the North Sea indicated that the temperature difference between injected CO_2 and the formation could generate significant thermal stresses at the cement-casing interface; however, the deep in-situ stress field partially mitigated the risk of interfacial debonding (Thompson et al., 2021).

Consequently, wellbore leakage constitutes one of the most significant engineering risks in CO_2 geological storage systems, with underlying mechanisms characterized by complex multi-factor coupling. Future efforts should focus on continuously strengthening well abandonment protocols, developing corrosion-resistant materials, improving cementing quality, and advancing multi-physical numerical modeling to enhance the long-term sealing reliability of wellbores.

3.2.4 Coupling of Multi-Physicochemical Processes and Leakage Evolution

Interfacial phenomena at the pore scale constitute the fundamental reactive unit in CO_2 geological storage systems. Injected CO_2 initially dissolves into the pore fluid, inducing acidification, and subsequently reacts with mineral surfaces, triggering dissolution-precipitation processes that modify key parameters such as porosity, permeability, and tortuosity. The evolution of these microstructures governs not only CO_2 migration and trapping efficiency within the reservoir but also directly affects the integrity of the caprock and wellbores. When pore-scale reactions propagate temporally and amplify spatially to the reservoir and site scales, they can manifest as characteristic leakage pathways and modes. Examples include diffuse leakage caused by caprock weakening, channelized leakage along reactivated faults, and vertical leakage following cement carbonation in wellbores. Therefore, understanding and characterizing water- CO_2-rock interactions at the pore scale is fundamental to elucidating the long-term stability of carbon storage systems and their potential leakage mechanisms (White et al., 2005; Gaus et al., 2005; Gaus, 2010; Molins et al., 2014).

In deep saline aquifers, CO_2 solubility is primarily governed by temperature, pressure, and salinity. The resulting acidification induces dissolution followed by reprecipitation of carbonate, sulfate, and aluminosilicate minerals. These reactions buffer or enhance acidity, thereby modifying pore structures and solute transport properties. Carbonate minerals react relatively rapidly, influencing system behavior during early injection stages, whereas feldspars and clays react more slowly, typically requiring geological timescales to produce significant effects (White et al., 2005). Such water- CO_2-rock reaction processes ultimately govern the long-term sealing capacity of both the reservoir and the caprock (Fig. 12).

$CO_2$2-water-rock interactions are commonly represented using reactive transport models (RTMs). These models are generally classified into two categories: continuum-scale and pore-scale models. Continuum-scale models are primarily employed for site-scale risk assessment and long-term prediction, whereas pore-scale models focus on microscopic dissolution-precipitation mechanisms. Combining these approaches enables cross-scale characterization: pore-scale models reveal fundamental mechanisms, whereas continuum-scale models are employed for risk prediction. However, key parameters, including reactive surface area and kinetic constants, carry substantial uncertainties, directly influencing predictions of leakage modes

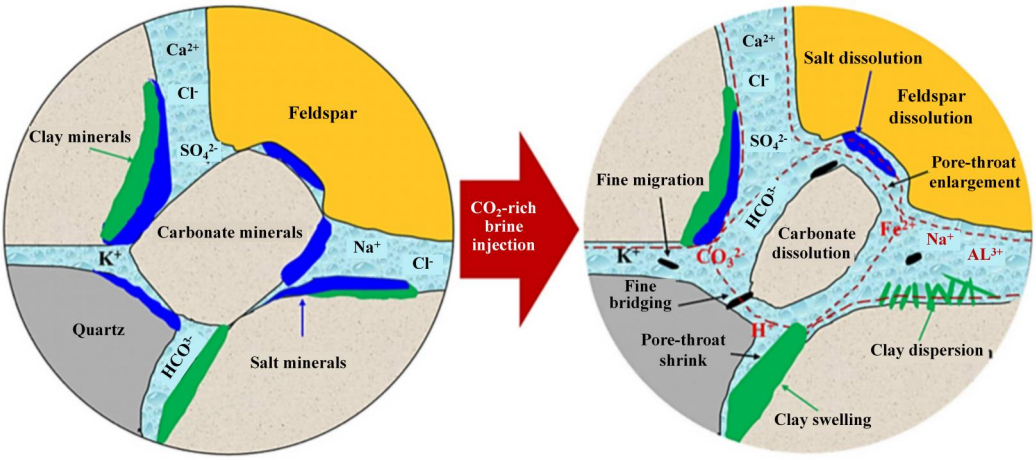

Fig. 12 Process of CO_2 -water-rock reaction (Tan et al., 2025)

(Lasaga et al., 1994; Palandri & Kharaka, 2005; Zheng et al., 2009). If mineral reactions modify the pore network within the caprock, even slow diffusion processes may evolve into CO_2 leakage pathways.

Geological CO_2 storage represents a classical Thermo-Hydro-Mechanical-Chemical (THMC) coupled process. CO_2 injection induces increased pore pressure and reduced effective stress, accompanied by temperature gradients and mineral reactions. These processes modify porosity, permeability, and rock mechanical properties, thereby influencing CO_2 migration and storage integrity. Simulations indicate that mineral dissolution may reduce the shear modulus of the caprock, increasing fracture risk, while fluid pressure buildup can propagate along faults or the wellbore-caprock interface, forming leakage conduits. Consequently, potential leakage modes in a storage system should be analyzed using an integrated multi-physical framework (Li et al., 2016; Gan et al., 2021; Fan et al., 2023).

3.3 Leakage Mode Classification and Summary of Characteristics

Based on the preceding analysis, leakage modes can be categorized according to pathway characteristics, leakage rate, and duration. These categories primarily include pore-type versus fracture-type, slow versus abrupt, continuous versus intermittent, and localized versus global leakage (Fig. 13).

Pore-type leakage refers to the slow, diffusive migration of CO_2 through microscopic pores within the rock matrix. It is commonly observed in deep saline aquifers or low-permeability reservoirs and is primarily controlled by porosity, permeability, and capillary pressure. This mode exhibits a low leakage rate but may persist over extended durations. In contrast, fracture-type leakage occurs along high-permeability conduits, such as faults and fractures, where CO_2 migrates rapidly under pressure gradients. This mode is typically associated with fault-developed zones or high-pressure injection scenarios and can result in significant CO_2 leakage over short periods.

From a dynamic perspective, slow leakage manifests as long-term, low-rate seepage, commonly associated with pore-type pathways. Although the instantaneous leakage rate is small, the long-term cumulative effect may be substantial. Abrupt leakage, however, is typically triggered by events such as fault reactivation, wellbore failure, or caprock fracturing. It is characterized by a sudden onset and high flow velocity, posing an immediate environmental risk. Continuous leakage refers to a stable, sustained release of CO_2 along a leakage pathway, commonly associated with pore-type or slow leakage modes. Intermittent leakage exhibits a periodic or conditionally triggered pattern, often associated with fractures or pressure fluctuations, resulting in significant variations in leakage rate.

Regarding spatial scale, localized leakage is confined to a single or a few point sources (e.g., a wellbore, a localized fault), with a limited area of impact but potentially high local concentrations. Global leakage involves extensive networks formed through multiple faults or fracture systems, posing a substantial threat to the overall sealing integrity of the storage system.

The characteristics delineated by this classification suggest distinct priorities for monitoring design and imply different risk profiles. Pore-type, slow, and diffuse leakage presents significant monitoring challenges due to its low signal strength; it requires long-term, high-sensitivity geochemical (e.g., groundwater composition) and pressure monitoring in overburden aquifers. Fracture-type, abrupt, and localized leakage (e.g., from a wellbore), while high-risk, often yields clearer signals such as rapid pressure changes, microseismic activity, or focused soil gas anomalies, enabling detection with wellhead instruments, seismic arrays, and targeted surface surveys.

In summary, the features most prone to CO_2 leakage are concentrated in wellbores (e.g., seal failure) and faults or fractures (e.g., fracture propagation induced by natural or triggered seismicity, or interactions between the reservoir/caprock and pre-existing faults). In contrast, molecular diffusion through intact rock matrices is an extremely slow process and typically becomes a practical leakage concern only if the diffused CO_2 subsequently enters higher-permeability pathways, such as fractures. It is crucial to emphasize that CO_2 leakage rarely occurs via a single mode and often involves multiple mechanisms:

(1) supercritical CO_2 may undergo viscous fingering or channeling along high-permeability pathways;

(2) driven by buoyancy, CO_2 may ascend rapidly through fractured conduits;

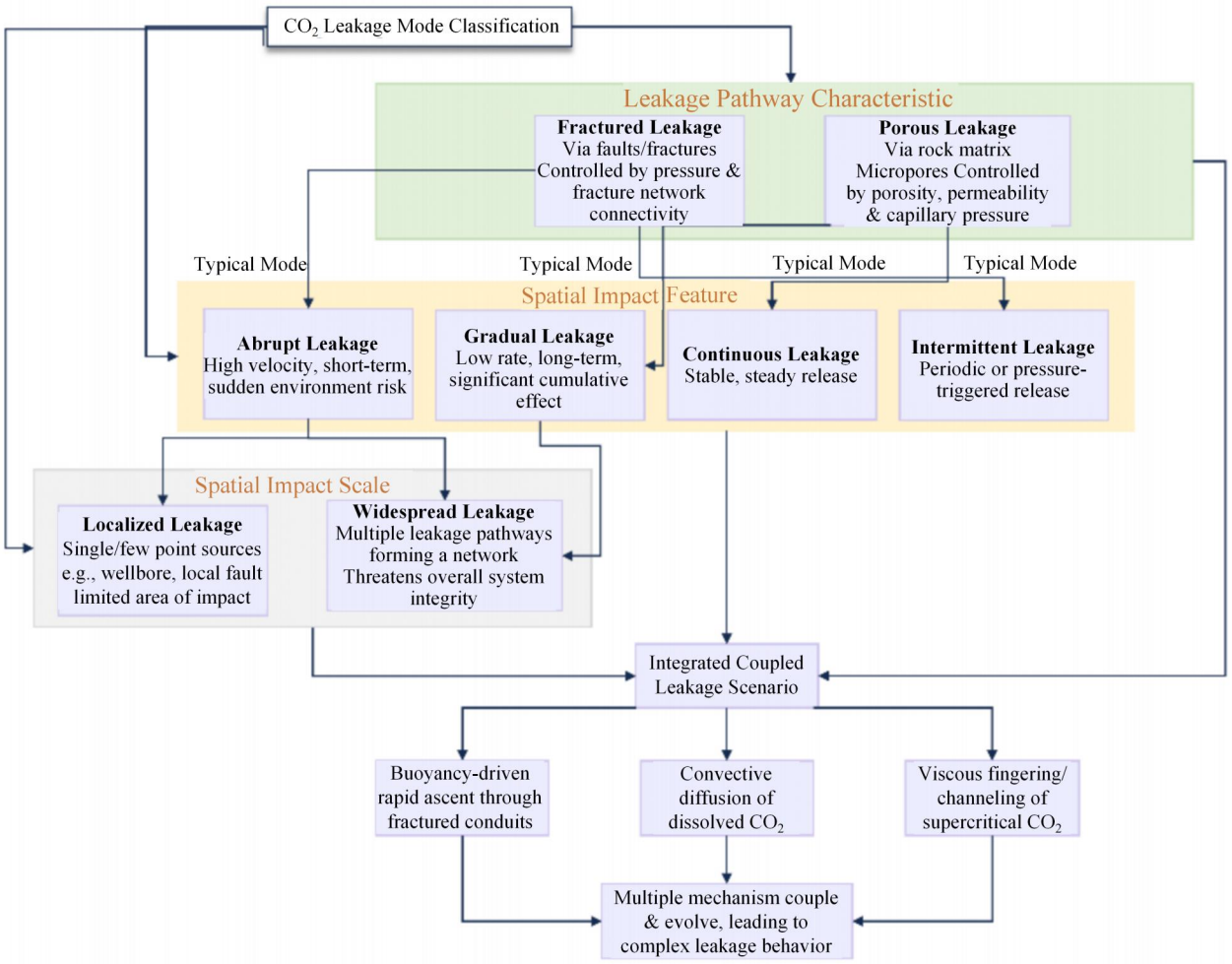

Fig. 13 Classification and Characteristics of CO_2 Geological Sequestration Leakage Models

(3) a portion of CO_2 dissolved in formation water may migrate gradually through convective mixing and diffusion. These mechanisms may interact and evolve over time, resulting in complex leakage behaviors.

4 Leakage and Sealing: Multiscale Definitions and Dynamics

4.1 Definitions of Leakage and Sealing

Leakage and sealing are fundamental concepts in evaluating the safety of storage systems in geological CO_2 storage research. Existing definitions primarily derive from general dictionaries or regulatory documents. For instance, the Encyclopædia Britannica defines leakage as "the accidental escape of a substance through a crack or hole"; the Contemporary Chinese Dictionary describes it as "the flow of liquids, gases, etc., through gaps or holes, typically referring to physical leakage"; and the EU Directive on the Geological Storage of Carbon Dioxide (2009/31/EC) defines it as "any release of CO_2 from the storage complex", in which the storage complex encompasses not only the reservoir but also the caprock and surrounding formations that affect overall storage integrity (Fig. 14). This broader definition extends beyond the notion of a simple "escape through holes", yet it fails to distinguish internal migration within the reservoir from leakage occurring after breaching the system boundary. While they possess a degree of universality, these definitions are hindered by three critical operational limitations:

(1) lack of pore-to-basin scalability,

(2) ambiguity between internal migration and boundary-breach failure,

(3) absence of measurable metrics to support engineering and regulatory decisions.

As a result, they may inadequately represent the multiscale nature of CO_2 storage and can risk conflating the distinct processes of migration, transformation, and leakage.

From the perspective of geological CO_2 storage, defining leakage merely as "escape" is insufficient. The behavior of CO_2 in the subsurface is primarily characterized by migration—namely, its movement and redistribution within the reservoir driven by pressure gradients, buoyancy, and permeability. This migration can induce changes in phase state or distribution, thereby resulting in different trapping modes, that is, transformation processes such as the transition from a free phase to a dissolved or mineral phase. Leakage occurs when CO_2 breaches the boundary of the storage unit and subsequently enters non-target zones. Correspondingly, sealing denotes the long-term capacity of the reservoir, caprock, and associated geological

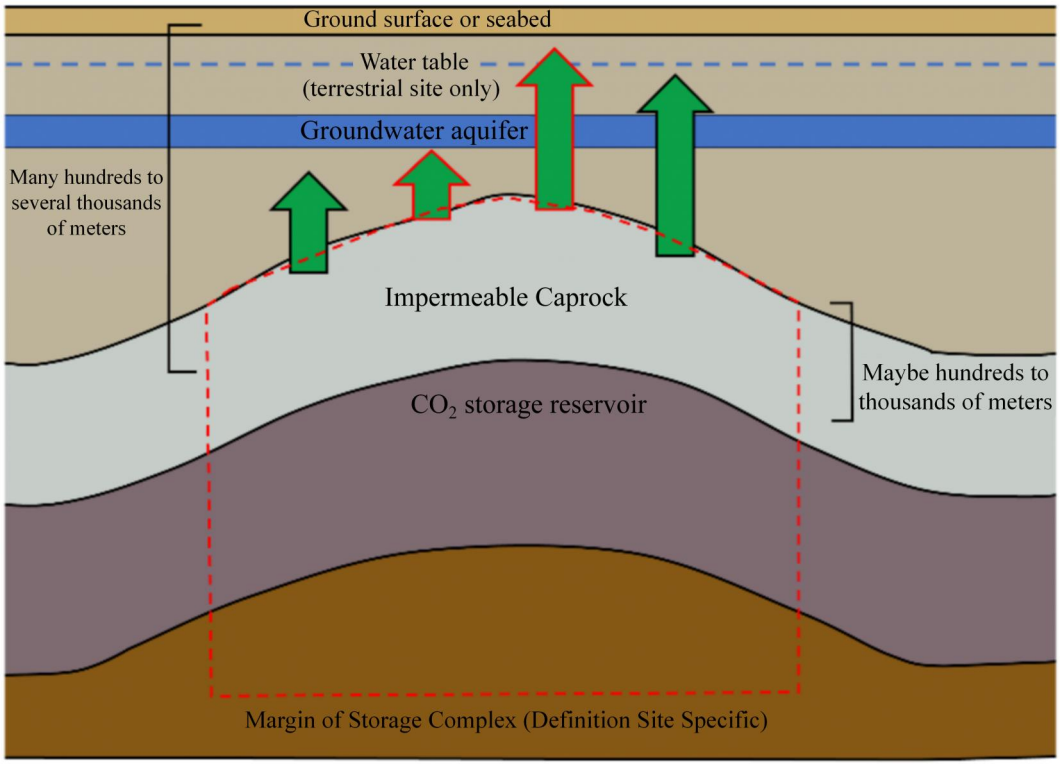

Fig. 14 Schematic illustration of a CO2 storage complex and the meaning of leakage in accordance with the EC Storage Directive (EC, 2009)

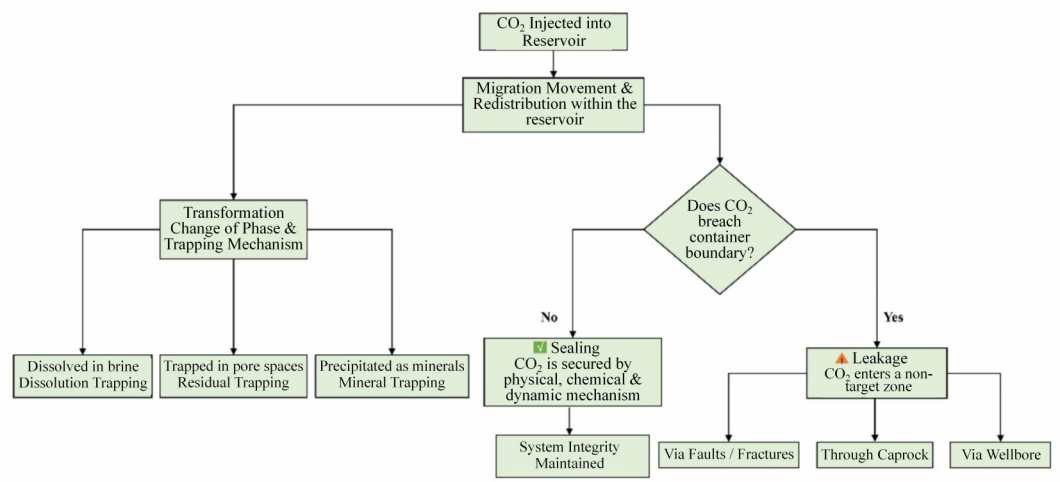

Fig. 15 Migration, Transformation, and Boundary Breakthrough in Geological CO_2 Storage

formations to confine and impede CO_2 through physical, chemical, or dynamic mechanisms, with its primary function being the maintenance of storage system integrity (Bryant et al., 2008; Rutqvist, 2012)(Fig. 15).

To establish a precise and operational multiscale definitional framework, this study proposes an analytical approach centered on the Object-Process-Boundary (OPB) concept, emphasizing that the determination of leakage and sealing at different scales must be grounded in the boundaries of the corresponding system (Fig. 16). This framework emphasizes the following principles: Migration denotes the internal movement and redistribution of CO_2 within a defined scale, without breaching the system boundary of that scale. Leakage denotes the process by which stored CO_2 breaches the system boundary of its sealing unit. Critically, "breach" is defined by a quantifiable condition where the driving forces (e.g., pressure, buoyancy) exceed the resistance forces (e.g., capillary entry pressure, fracture strength) at the boundary. Sealing denotes the capacity of physical, chemical, or mechanical mechanisms to prevent this breach. It is crucial to underscore that leakage adopts "boundary breach under defined force thresholds" as its unified criterion, sealing embodies "boundary maintenance quantified by maximum resistance metrics" as its core function, and migration represents a dynamic process confined within the boundary.

To operationalize these principles, a clear boundary selection protocol and corresponding measurable engineering metrics are required for each scale. Boundaries are selected based on their primary function:

(1) Structural boundaries (e.g., caprock geometry) for physical confinement;

(2) Dynamic boundaries (e.g., pressure front, monitored plume extent) based on system behavior and monitoring capability; and

(3) Regulatory/Protective boundaries (e.g., base of underground sources of drinking water) defined by safety regulations.

The selection dictates the relevant leakage indicators and sealing metrics. This unified criterion can be systematically applied across hierarchical levels—pore, core, reservoir, site, and basin (Table 5).

To be specific, at the pore scale, the movement of CO_2 within the pore network constitutes migration; breaching a pore-throat boundary occurs when the local capillary pressure exceeds the capillary entry pressure ($P_c > P_{ce}$), representing leakage; and immobilization by capillary threshold pressure constitutes sealing, quantified by P_{ce} and residual saturation. At the core scale, migration occurs within the REV; leakage is indicated by a sustained CO_2 flux across the REV boundary, measurable in core-flood experiments. At the reservoir scale, migration occurs beneath the caprock; leakage is signaled by CO_2 saturation at the caprock interface (via seismic) or when formation pressure exceeds the fracture gradient (e.g., > 0.85 of the minimum principal stress, σ_3). At the site scale, migration is within the monitored domain; leakage is confirmed by detecting CO_2 (e.g., via tracers) outside the monitored boundary or above regulatory concentration limits in protected aquifers. At the basin scale, leakage constitutes a surface flux exceeding natural baselines or groundwater chemistry anomalies beyond designated zones (Fig. 17). In summary, this operational OPB framework transforms qualitative concepts into a decision-support tool. It provides the essential logical link within the "Monitoring-Prediction-Regulation-Intervention" closed-loop management system: monitoring data are evaluated against the scale-specific boundaries and metrics defined here to classify system state, which in turn triggers predictive modeling and, if necessary, regulatory or intervention actions.

Multiscale sealing processes act in opposition to leakage. Sealing can be understood as the set of restriction mechanisms acting on CO_2 prior to its breaching a boundary. These mechanisms are commonly categorized into four types: (i) Structural and capillary sealing, controlled by impermeable caprocks and capillary threshold pressures, which prevent further upward migration of CO_2 (Shukla et al., 2010); (ii) Residual sealing, in which CO_2 is trapped as disconnected ganglia by capillary forces within pore spaces (Bachu, 2003); (iii) Solubility sealing, whereby CO_2 dissolves into the formation water and the resulting denser brine may sink (Ennis-King & Paterson, 2002); and (iv) Mineral sealing, in which CO_2 reacts with host rock minerals to form stable carbonate solids, thereby enabling long-term storage (Egermann et al., 2005). Additionally, other mechanisms, such as pressure sealing and concentration sealing, have been proposed in various studies, often acting in superposition with capillary sealing to collectively form resistance barriers. It is important to note that "trapping mechanisms" describe the long-term fate of CO_2, whereas "sealing capacity" emphasizes the immediate effectiveness in preventing boundary breaches; the two are complementary but conceptually distinct. Furthermore, the characterization of sealing capacity should be based on quantifiable indicators with clear physical significance, such as breakthrough pressure and maximum sealing pressure. This approach not only facilitates the unification of a cross-scale sealing evaluation framework but also provides a robust basis for risk prediction and engineering design.

To transition from a conceptual schema to an actionable tool, this OPB framework is designed to integrate directly with the "Monitoring–Prediction–Regulation–Intervention" management cycle (Section 5). It provides the critical decision logic by establishing scale-specific, measurable criteria for a "boundary breach". For instance, at the reservoir scale, leakage is operationally defined by monitoring data satisfying criteria such as CO_2 saturation at the caprock interface (from seismic) or formation pressure exceeding a defined fraction of the fracture gradient. This creates a direct mapping from monitoring variables (e.g., pressure anomalies, tracer presence, geochemical shifts) to the binary classification of system state (migration vs. leakage). When such criteria are met, it triggers a state reclassification within the management system, activating the subsequent "prediction" (model updating and forecasting) and "regulation/intervention" modules. Thus, the OPB framework furnishes the essential, quantifiable thresholds that enable the closed-loop system to function not merely as a conceptual diagram but as a responsive control logic.

The multiscale definitional framework proposed in this section not only addresses the shortcomings of existing definitions but also establishes a more rigorous and operational conceptual system by clarifying the interrelationships among migration, transformation, leakage, and sealing. This framework emphasizes the boundary conditions of leakage, highlights the multiple mechanisms of sealing, and provides theoretical support for subsequent leakage risk modeling, monitoring technology development, and management strategies.

4.2 Driving and Resisting Forces in CO_2 Migration and Sealing

The migration and sealing of CO_2 in subsurface geological formations fundamentally represent a dynamic balance between driving forces that promote migration and resisting forces that ensure sealing across multiple scales (Bachu et al., 1994; Lindeberg & Wessel-Berg, 1997; Celia et al., 2005). To clarify the interaction, it is essential to distinguish the fundamental driving forces (e.g., buoyancy, pressure gradient), the physical-chemical processes they induce (e.g., two-phase flow, geomechanical slip, dissolution), and the key properties or thresholds that govern the outcome of these processes (e.g., capillary entry pressure, fracture gradient, friction coefficient). Driving mechanisms constitute the primary sources of CO_2 mobility and include:

(1) Buoyancy Drive: The density of supercritical CO_2 is 30–50% lower than that of brine, making buoyancy the dom-

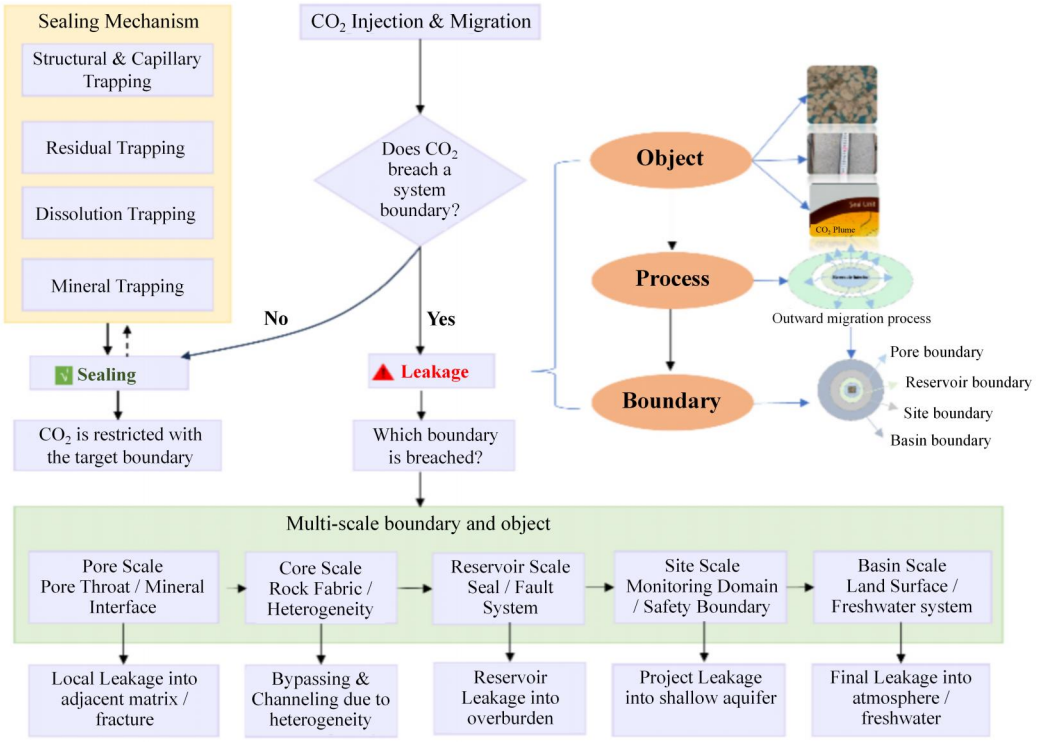

Fig. 16 A Multi-Scale Object-Process-Boundary (OPB) Framework for Defining CO2 Leakage and Sealing

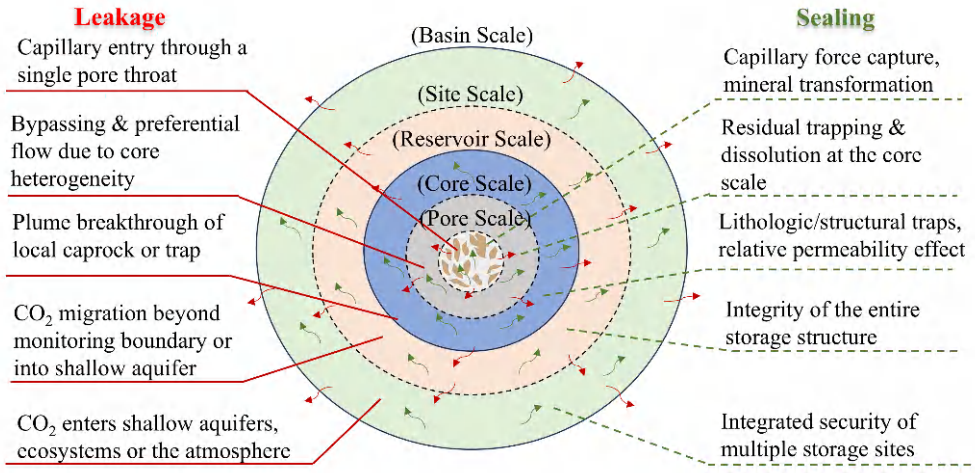

Fig. 17 Conceptual Framework of Multi-scale CO_2 Leakage and Sealing

inant force for upward migration toward the caprock. The dominance of buoyancy over capillary trapping can be assessed by the dimensionless Bond number $B_0 = \Delta\rho g k/(\gamma \cos\theta)$. For typical storage conditions (P > 8 MPa, T = 30–50°C, salinity < 5 mol/kg), the large density contrast ($\triangle\rho$) ensures $B_o \gg 1$ in high-permeability zones, driving vertical migration. In contrast, in low-permeability caprocks, $B_o \ll 1$, and capillary forces dominate, inhibiting flow.

(2) Pressure Gradient: The excess pressure generated during injection facilitates radial plume expansion and helps overcome local capillary entry resistance.

(3) Natural Hydraulic Gradient: Regional groundwater flow dictates the migration pathways and velocities of CO_2 plumes (Evans, 2013).

(4) Stress perturbations can reactivate faults or fractures, generating new leakage conduits.

(5) Although slow, diffusion along concentration gradients allows CO_2 to penetrate caprock micropores and dissolve into groundwater, influencing long-term storage security (Johnson et al., 2005).

Resisting mechanisms represent the constraints on CO_2 migration imposed by various physical and chemical processes,

primarily including capillary resistance, viscous effects, chemical reactions, and mineral precipitation (Geloni et al., 2011; Dashtian et al., 2019). The efficacy of each mechanism is quantified by specific, measurable parameters: capillary resistance by the capillary entry pressure, geomechanical resistance by the fault reactivation pressure derived from the Mohr-Coulomb criterion, and chemical resistance by reaction kinetics and thermodynamic equilibria. These parameters, whether measured in the lab or inferred from field tests, form the basis for defining sealing thresholds. A critical aspect for practical risk assessment and storage security is the characteristic time scale over which each resistance mechanism dominates, ranging from immediate (short-term) barriers to gradual (long-term) immobilization processes. Geological heterogeneities, such as low-permeability mudstone lenses and barriers, can also prevent the upward breakthrough of the plume, forcing it to spread laterally and become immobilized in structural or stratigraphic traps (Doughty et al., 2001; Flett et al., 2005). Specifically, the capillary entry pressure of a tight caprock is the first and most crucial barrier resisting CO_2 buoyancy and preventing its seepage into the caprock (Ajayi et al., 2019; Ding et al., 2023). This capillary resistance acts as the primary short-term (operational to decadal scale) sealing mechanism. When the CO_2 pressure (P_{CO_2}) is lower than the capillary entry pressure (P_c) of a pore throat, it becomes immobilized at the throat, preventing further migration. Similarly, in deep saline aquifers, when CO_2 cannot enter a brine-saturated capillary barrier—i.e.,$P_{CO_2} - P_{brine} < P_c$, where P_{brine} is the brine pressure—the resulting fluid displacement mechanism leads to "snap-off" trapping of CO_2 (Saadatpoor et al., 2009). Conversely, CO_2 will migrate into the overlying rock if the condition is not met. When sufficient brine is displaced to exceed the percolation threshold, a continuous flow path for CO_2 becomes established within the pore system.

Capillary effects are strongly coupled with viscous forces. The viscosity contrast between CO_2 and brine often induces unstable fingering during displacement, fragmenting the plume into smaller clusters. This enhances residual trapping by increasing the volume of immobilized CO_2. Both capillary and viscous (hydrodynamic) resistances are dominant during the injection and early post-injection phases, providing essential short- to medium-term security. Additionally, CO_2 dissolution into formation brine produces weak carbonic acid, initiating mineral-fluid reactions (Brantley & Conrad, 2008; Gysi & Stefánsson, 2012; Kanakiya et al., 2017). Dissolution not only increases storage density but also provides the reactive basis for subsequent mineral trapping, where CO_2 precipitates as stable carbonate minerals (De Silva et al., 2015; Ma et al., 2020). Solubility trapping strengthens over decades to centuries, while mineralization represents the most secure long-term (centennial to millennial scale) sealing mechanism, although localized precipitation may clog pore throats, reducing permeability and impairing injectivity (Gunter et al., 1993; Liu et al., 2011; Sbai & Azaroual, 2011; Cho et al., 2019). Thus, the resistance system operates as a dynamic sequence: robust short-term physical barriers (capillary, viscous) are paramount for initial integrity, effectively "buying time" for the slower-acting chemical processes (dissolution, mineralization) to develop and ultimately provide permanent storage security.

The relative dominance of driving and resisting forces varies across scales. At the pore scale, capillary entry pressures and surface chemical reactions control local CO_2 distribution. At the reservoir scale, buoyancy, injection pressure, and heterogeneity jointly determine plume migration and immobilization. At the site scale, well placement, injection strategies, and regional hydraulic conditions constrain plume evolution, making reservoir engineering measures (e.g., injection rate management, pressure control) essential for enhancing resistance and mitigating leakage risk.

4.3 Multiscale and Multidimensional Variations in Driving and Resisting Force Attenuation

The preceding sections have discussed the processes of CO_2 leakage and sealing in geological reservoirs with respect to driving and resisting forces. However, these mechanisms vary significantly across spatial scales and modeling dimensions; their effects are not linearly additive but instead exhibit systematic attenuation or amplification as scale increases. This section examines the evolutionary characteristics of these forces across three primary scales—pore–core, reservoir–fault–caprock, and regional–basin—while also considering dimensional effects.

At the pore–core scale (μm–cm), CO_2 migration is primarily governed by capillary forces and mineral reactions. Capillary trapping results in residual fluid saturation, while mineral dissolution–precipitation occurs within pore throats and microfractures, potentially exerting both beneficial and detrimental effects on permeability. The size and distribution of pore structures determine the efficiency of capillary resistance, whereas reaction rates and precipitation sites control the persistence and stability of chemical trapping. At this scale, resisting mechanisms exert a strong attenuating effect on driving forces, significantly restricting CO_2 migration during the early stages.

At the reservoir–fault–caprock scale (m–km), the dominant factors controlling driving and resisting forces change. Stratigraphic heterogeneity, fracture network connectivity, and fault sealing capacity collectively determine CO_2 migration patterns within the reservoir. Faults and fractures may function either as sealing barriers or leakage conduits, with their dual role governed by breakthrough pressure and the presence of clay gouge. At this scale, attenuation of driving forces depends largely on resistance provided by structural trapping and lithological contrasts. However, once a highly connected fracture network forms, it can rapidly reduce the effectiveness of resistance, enabling CO_2 to breach reservoir sealing through a pipeline-flow mode.

At the regional–basin scale (km–100 km), macroscopic tectonic controls constitute the decisive factors for sealing and leakage. Tectonic features such as folds, anticlines, and rift basins frequently form large-scale traps, allowing CO_2 to accumulate beneath caprocks under buoyancy forces. At this scale, resisting mechanisms manifest as the macroscopic integrity of caprocks and the ultimate constraint imposed by their breakthrough pressure. Once a critical pressure threshold is exceeded, leakage may occur in a sudden and catastrophic manner. Conversely, driving forces at this scale are modulated by the

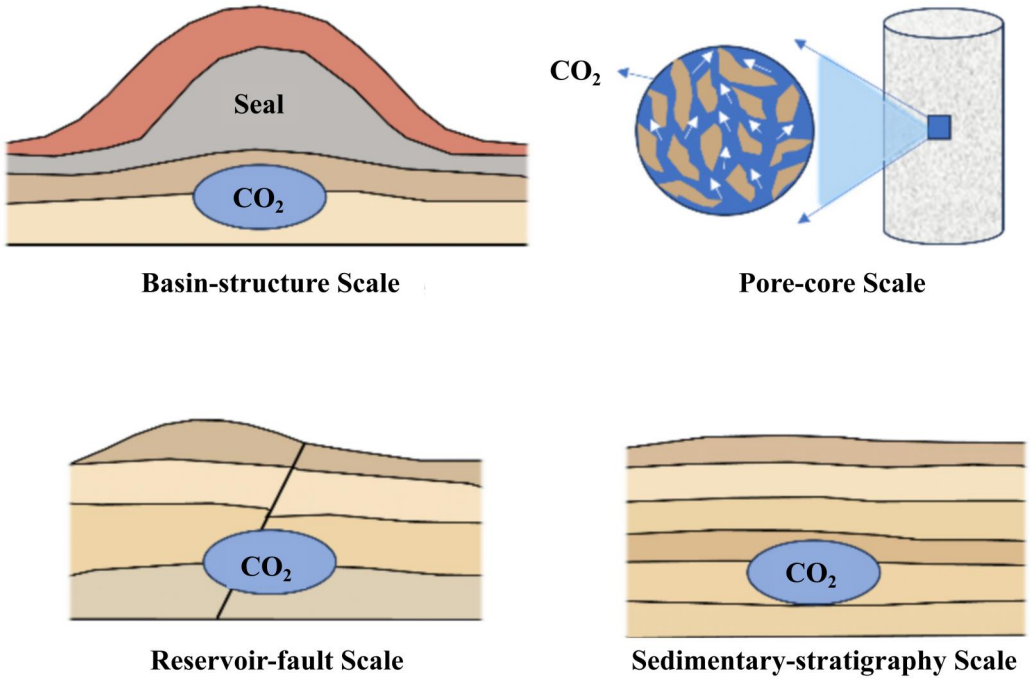

Fig. 18 Conceptual Diagram: Multi-Scale and Multi-Dimensional Differences in Geological CO_2 Storage

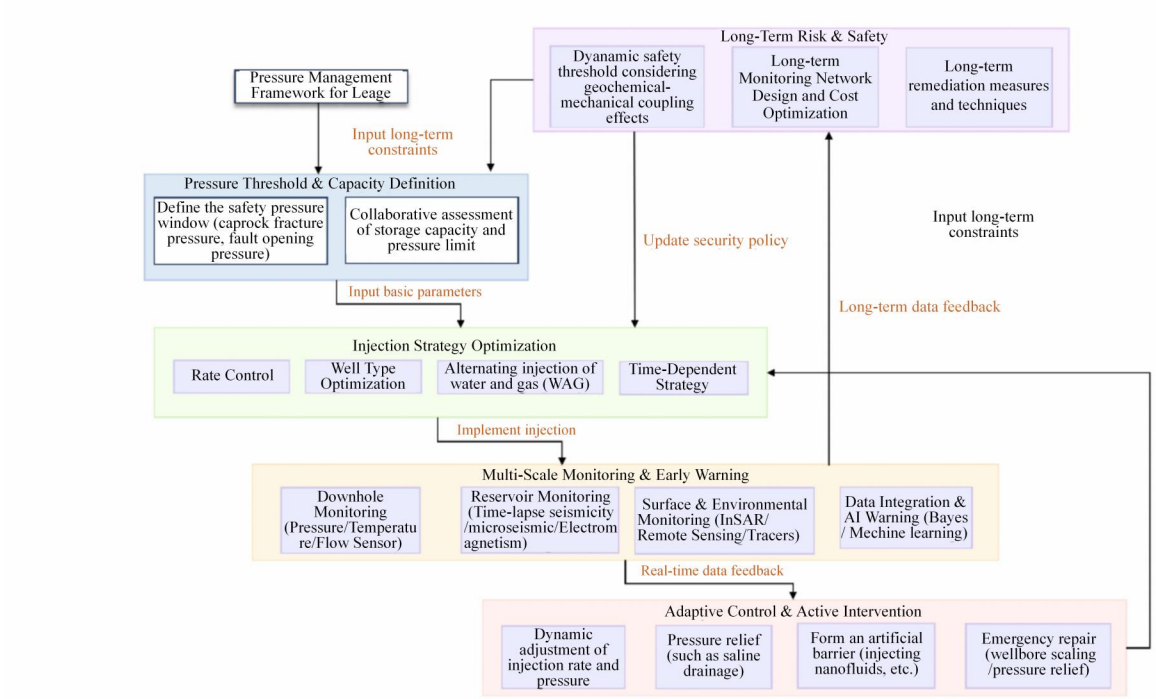

Fig. 19 A Framework for Leakage-Oriented Pressure Management in Geological CO_2 Storage

basin's thermo-fluid environment, and their attenuation exhibits strongly nonlinear characteristics (Fig. 18).

It is important to note that the scale dependence of key parameters further complicates the behavior of resisting and driving forces. For instance, field-scale feldspar dissolution rates are frequently several orders of magnitude lower than laboratory measurements, whereas diffusion coefficients and hydraulic conductivity generally increase with scale. This implies that direct application of laboratory data to field-scale predictions may lead to significant deviations, necessitating integration through upscaling methods (e.g., fractal geometry, method of moments). Furthermore, dimensionality is particularly critical in leakage simulations. Two-dimensional (2D) models frequently underestimate lateral dispersion and leakage risks, whereas three-

dimensional (3D) models offer a more realistic representation of CO_2 migration pathways within complex fault and anticline structures. The presence of fractures may transform dispersed flow into an approximately one-dimensional (1D), high-velocity channelized flow, substantially weakening resisting mechanisms and accelerating the dominance of driving forces. Neglecting the 3D structure of faults and fractures in simulations may result in over- or underestimation of sealing efficiency, thereby compromising the reliability of storage security assessments.

Therefore, attenuation of resisting and driving forces in geological CO_2 storage exhibits significant dependence on both scale and dimensionality: capillary forces and mineral precipitation provide the primary resistance at the pore–core scale; heterogeneity and fault sealing capacity control leakage risk at the reservoir–fault scale; and tectonic trapping and caprock integrity govern overall security at the regional–basin scale. Concurrently, systematic differences between 2D and 3D simulations highlight the need to enhance predictive accuracy through integrated multiscale and multidimensional approaches. This necessitates explicit guidance on model application: Two-dimensional simulations are generally inadequate for quantifying leakage risk, as they cannot capture the lateral connectivity and complex, channelized flow pathways (e.g., through fracture networks) that critically control leakage. A credible 3D assessment must, at minimum, incorporate the geometry of major faults and conceptualize fracture network connectivity based on site data. Neglecting 3D effects risks false-negative leakage predictions, while oversimplifying connectivity may lead to false-positive risk overestimates (Table 6). In CO_2 storage safety assessments and risk management, reliance on single-scale or simplified models should be avoided. Instead, a coupled methodology integrating multi-parameter upscaling with multidimensional numerical simulation should be adopted. This approach provides not only a more comprehensive understanding of the evolution of resisting and driving forces but also a theoretical foundation for future research on leakage control and remediation technologies.

5 A Pressure Management Framework for Leakage Mitigation

Building upon the preceding analysis of multiscale leakage and sealing dynamics, it is evident that pressure perturbation induced by injection is a core factor in triggering leakage risks. Excessively high reservoir pressure may lead to caprock fracturing or fault reactivation, thereby creating highly conductive leakage pathways. Consequently, establishing an active control framework focused on pressure management is crucial for ensuring the long-term safety of CO_2 storage (Rutqvist, 2012; Adisornsupawat et al., 2024). This section synthesizes existing research and proposes a closed-loop pressure management framework— "Monitoring–Prediction–Regulation–Intervention"—to achieve lifecycle risk control in CO_2 storage.

(1) Defining Pressure Thresholds and Storage Capacity

Effective pressure management requires defining the safe operating window of the reservoir–caprock system. Its upper limit is typically governed by two critical pressures: the caprock breakthrough pressure, defined as the minimum capillary pressure required for the non-wetting phase to enter caprock pores (Ajayi et al., 2019), and the fault/fracture opening pressure, which depends on fault gouge properties and infill strength (Guglielmi et al., 2017). To translate these concepts into actionable engineering thresholds, explicit geomechanical criteria must be applied. The caprock integrity limit should be assessed against the minimum principal stress criterion to prevent hydraulic fracturing, while the fault reactivation limit must be evaluated using the Mohr-Coulomb failure criterion (or slip tendency analysis) to prevent shear slip. In practice, the maximum allowable injection pressure must be maintained below the lower of these two values (Adisornsupawat et al., 2024). Standard practice typically involves maintaining injection pressure below 90% of the fracturing pressure to prevent formation failure, which represents one form of incorporating an operational pressure margin. A comprehensive margin should also account for uncertainties in in-situ stress, rock properties, and model predictions. However, operational protocols must consider thermo-hydro-mechanical (THM) coupling effects induced by cold fluid injection, which can generate new fracture networks in the reservoir, effectively lowering the safe threshold. Furthermore, a coupling exists between injectivity and pressure thresholds: higher injection rates can increase short-term storage capacity but may also induce overpressure and elevate leakage risks (Calabrese et al., 2005). Therefore, capacity assessments should be performed in conjunction with pressure limits to ensure efficient reservoir utilization without breaching structural sealing thresholds.

(2) Injection Strategy Optimization

The injection strategy constitutes the primary means of pressure management, aiming to enhance storage efficiency while preventing localized overpressure. Studies indicate that lower injection rates facilitate CO_2 accumulation at the reservoir base and its dissolution into formation water, thereby mitigating pressure buildup, whereas excessively high rates promote channeling through high-permeability pathways, reducing storage efficiency (Calabrese et al., 2005). Simulation results suggest that horizontal wells outperform vertical wells in reducing pressure concentration and mitigating fault reactivation risks (Zhang & Agarwal, 2012). Moreover, Water-Alternating-Gas (WAG) injection promotes CO_2 dispersion and fingering within the reservoir, enhancing residual trapping and attenuating continuous gas-phase migration (Chaturvedi et al., 2021). Recent time-dependent strategies emphasize immediate brine displacement after CO_2 injection to rapidly convert mobile CO_2 into the residual phase and accelerate solubility trapping, thereby significantly reducing leakage potential (Huber et al., 2016). These findings suggest that comprehensive pressure management—through rate control, well placement optimization, and alternate injection—can achieve controllable reservoir pressure and safe storage under varying conditions.

(3) Multiscale Monitoring and Geomechanical Model-Based Prediction

The dynamic evolution of the pressure field and its influence on leakage must be monitored in real time. Wellbore monitoring

constitutes the first line of defense, encompassing wellhead pressure and flow meters, fiber-optic pressure/temperature sensors, and cement bond logs, which are employed to identify well integrity issues (Lippmann et al., 2007). At the reservoir scale, time-lapse seismic, microseismic, electromagnetic, and gravity monitoring are extensively utilized to observe CO_2 plume migration and pressure perturbations (Chadwick et al., 2009). At the surface and environmental level, InSAR and fiber-optic sensing detect surface deformation induced by pressure changes, whereas hyperspectral remote sensing and tracer detection can directly identify leakage signals (Ajayi et al., 2019).

The critical link between monitoring and actionable insight is provided by geomechanical models. Poroelastic and coupled THM models translate monitored data (e.g., pressure, deformation) into quantitative updates of the subsurface stress field and failure risk. For instance, semi-analytical workflows based on layered poroelasticity can efficiently compute stress changes induced by distributed pressure and temperature variations, accounting for caprock-reservoir contrasts and undrained conditions—a significant advantage for rapid assessment and screening (Zhai et al., 2024). For detailed near-well analysis, such as leakage through a compromised wellbore with material heterogeneities, full coupled finite element models are essential. The accuracy of such models depends critically on the selection of primary variables (e.g., the capillary pressure-gas pressure (PP) scheme versus the liquid pressure-gas saturation (PS) scheme) and coupling algorithms (monolithic vs. sequential), especially at interfaces between different materials like cement, steel, and rock (Islam et al., 2020). Integrated analysis increasingly utilizes these calibrated models with Bayesian inference and machine learning techniques to assimilate real-time data, reduce uncertainty, and enable dynamic risk forecasting (Jackson et al., 2024; Liu et al., 2024). Thus, monitoring coupled with robust geomechanical prediction forms the intelligent core of the management framework.

(4) Adaptive Regulation, Stress Management, and Active Intervention

Based on monitoring data, pressure management should incorporate capabilities for real-time regulation and active intervention. Dynamic adjustment of injection rates and pressures constitutes the most direct method to maintain reservoir pressure below the safe threshold (Gholami et al., 2021). For targeted mitigation of localized overpressure and stress perturbations, more specific strategies are employed. Pressure relief wells can be strategically deployed to extract formation brine in overpressured zones, directly reducing pore pressure and thereby increasing the effective stress on seals and faults to prevent their activation (Javadpour & Nicot, 2011); their placement and extraction rates are optimized using geomechanical models. Co-injection strategies, including Water-Alternating-Gas (WAG), serve a dual purpose: beyond managing macroscopic pressure buildup, they mitigate near-wellbore thermal stresses and promote a more uniform pressure distribution, actively stabilizing the stress field. Geomechanical models are crucial for optimizing the co-injection ratio and scheduling. Furthermore, controlled micro-fracturing, though primarily a diagnostic tool, can be engineered to create localized, conductive pathways within the reservoir rock itself. This acts as a deliberate "stress buffer," dissipating concentrated pressure that might otherwise load critical faults, but requires precise geomechanical design to ensure sealing. When monitoring and models indicate the development of potential leakage pathways, proactive measures such as injecting fluids that induce mineral precipitation or applying nanofluids to enhance sealing can be deployed to form artificial barriers (Vialle et al., 2016; Rathnaweera & Ranjith, 2020). In the event of a leakage incident, emergency measures include wellbore plugging (e.g., squeeze cementing, sidetracking), pressure relief, and the injection of sealing or repair materials. Consequently, the pressure management framework must incorporate dual functionalities: preventive regulation and emergency remediation.

(5) Long-term Risk Management and Security

CO_2 storage represents a long-term process spanning decades to millennia. Therefore, pressure management should not be confined to the injection phase but must extend throughout the entire lifecycle. Long-term risks primarily arise from geochemical–mechanical coupling effects; for instance, acidification may dissolve fracture fillings, reducing fault strength and dynamically lowering the safe pressure threshold (Raziperchikolaee et al., 2019). Consequently, the safe pressure window should be regarded as a dynamic parameter, necessitating continuous revision based on long-term monitoring. Simultaneously, the design of long-term monitoring networks must balance cost and accuracy, enabling rapid deployment of additional sensors upon detection of pressure anomalies. Regarding remediation, measures include both wellbore repair techniques and pressure dissipation or sealing technologies for fault or caprock leakage. Only through a continuous cycle of "Monitoring–Revision–Remediation" can the long-term security of geological CO_2 storage be ensured (Fig. 19).

In summary, the enhanced pressure and stress management framework for mitigating leakage incorporates five core, interlinked components:

(1) Defining pressure thresholds for caprock fracturing and fault activation based on geomechanical experiments and numerical modeling;

(2) Implementing dynamic injection control through strategies such as rate control, well placement optimization, and alternating injection;

(3) Establishing an integrated monitoring system coupled with geomechanical models for prediction;

(4) Performing adaptive regulation, including specific stress control methods (e.g., relief wells, co-injection), and active intervention based on model forecasts;

(5) Extending pressure management throughout the long-term lifecycle, integrating dynamic risk revision and cost optimization to ensure complete lifecycle security.

This framework integrates geomechanical understanding, multiscale monitoring technologies, and intelligent control methods, embodying the closed-loop philosophy of "Monitoring–Prediction–Regulation–Intervention". It serves as a crucial safeguard for the long-term safe operation of large-scale geological CO_2 storage projects.

6 Conclusions

This paper reviews and synthesizes the current understanding of leakage and sealing in geological CO_2 storage from a multi-scale perspective, systematizing the conceptual framework and regulatory principles involved. The principal conclusions are summarized as follows:

(1) Clarification of Multi-Scale Definitions: Through a systematic analysis of storage and migration spaces across scales and of dominant leakage pathways, existing concepts are integrated within an "object–process–boundary" analytical framework. This framework serves to clarify the distinctions and relationships among migration, transformation, sealing, and leakage, and establishes consistent identification criteria across pore, reservoir, site, and basin scales. This synthesis addresses prevalent conceptual ambiguity and scale fragmentation in the literature. The operational application and validation of this unified analytical approach in specific field contexts remain a key direction for future research.

(2) Synthesis of Driving–Resisting Force Coupling: The interplay of forces governing CO_2 fate is analyzed and synthesized. Buoyancy, seepage forces, and pressure perturbations are identified as the primary drivers for upward migration, while capillary sealing, mineral reactions, residual trapping, and caprock integrity constitute the primary resisting mechanisms. The dynamic spatiotemporal balance between these forces is established as the fundamental determinant of permanent immobilization versus boundary breach and leakage.

(3) Elucidation of Multi-Scale Dependencies: The review elucidates the hierarchical dependencies across scales and dimensions. At the pore–core scale, capillary effects and chemical reactions are shown to govern residual and mineral trapping. At the reservoir–fault–caprock scale, heterogeneity, fracture connectivity, and fault sealing capacity emerge as the critical factors controlling migration pathways and leakage risks. At the basin–regional scale, macroscopic geological structures are recognized as the overarching controls on the spatial distribution of CO_2 and its long-term sealing.

(4) Integration of Pressure Management Principles: Injection-induced overpressure is highlighted as a critical risk factor. The review integrates key principles into a closed-loop "Monitoring–Prediction–Regulation–Intervention" concept centered on pressure management. This conceptual model underscores the importance of lifecycle risk control through threshold management, dynamic adjustment, and long-term monitoring, outlining a coherent pathway for risk management in large-scale storage projects.

The safety of geological CO_2 storage is contingent upon the dynamic balance between driving and resisting forces, the coherent understanding of multiscale sealing mechanisms, and the implementation of proactive pressure management strategies. Future research should prioritize the development of cross-scale multi-physics coupling models and the integration of intelligent monitoring with real-time control technologies. This evolution is essential to advance storage strategies from "passive response" towards "active prevention", thereby ensuring the long-term security of large-scale geological CO_2 storage.

Acknowledgements

The authors gratefully acknowledge the support of this work by the Key Projects of the Geology Joint Fund of the National Natural Science Foundation of China (U2344226).

Conflict of interest

The authors declare no competing interest.

References

Adamu B, Gholami R, Downey W, et al. 2019. A novel approach to determine across-fault leakage in CO_2 reservoirs. *Journal of Petroleum Science and Engineering*, **181**: 106227. doi:10.1016/j.petrol.2019.06.001.

Adisornsupawat K, Sangnimnuan A, Rabiabpo P, et al. 2024. Evaluation of caprock integrity with laboratory scale in situ CO_2 injection test. *ARMA US Rock Mechanics/Geomechanics Symposium*, ARMA D041S054R002. doi:10.56952/ARMA-2024-0671.

Ajayi T, Gomes JS, Bera A. 2019. A review of CO_2 storage in geological formations emphasizing modeling, monitoring and capacity estimation approaches. *Petroleum Science*, **16**: 1028–1063. doi:10.1007/s12182-019-0340-8.

Al Haddad S, Mancini EA. 2013. Reservoir characterization, modeling, and evaluation of Upper Jurassic Smackover microbial carbonate and associated facies in Little Cedar Creek field, southwest Alabama, eastern Gulf coastal plain of the United States. *AAPG Bulletin*, **97**(11): 2059–2083. doi:10.1306/07081312187.

Aminu MD, Nabavi SA, Rochelle CA, et al. 2017. A review of developments in carbon dioxide storage. *Applied Energy*, **208**: 1389–1419. doi:10.1016/j.apenergy.2017.09.015.

Appelo CAJ, Postma D. 2004. *Geochemistry, Groundwater and Pollution*, 2nd ed. CRC Press / Balkema. doi:10.1201/9781439833544.

Bachu S, Watson TL. 2009. Review of failures for wells used for CO_2 and acid gas injection in Alberta, Canada. *Energy Procedia*, **1**: 3531–3537. doi:10.1016/j.egypro.2009.02.146.

Bachu S. 2008. CO_2 storage in geological media: Role, means, status and barriers to deployment. *Progress in Energy and Combustion Science*, **34**: 254–273. doi:10.1016/j.pecs.2007.10.001.

Bachu S, Bennion B. 2008. Effects of in-situ conditions on relative permeability characteristics of CO_2-brine systems. *Environmental Geology*, **54**: 1707–1722. doi:10.1007/s00254-007-0946-9.

Bachu S, Bennion DB. 2009. Interfacial tension between CO_2, freshwater, and brine in the range of pressure from (2 to 27) MPa, temperature from (20 to 125) °C, and water salinity from (0 to 334 000) $mg \cdot L^{-1}$. *Journal of Chemical & Engineering Data*, **54**(3): 765–775. doi:10.1021/je800529x.

Bachu S. 2003. Screening and ranking of sedimentary basins for sequestration of CO_2 in geological media in response to climate change. *Environmental Geology*, **44**: 277–289. doi:10.1007/s00254-003-0762-9.

Bachu S, Gunter WD, Perkins EH. 1994. Aquifer disposal of CO_2: hydrodynamic and mineral trapping. *Energy Conversion and Management*, **35**(4): 269–279. doi:10.1016/0196-8904(94)90060-4.

Bai B, Li X, Wu H, et al. 2017. A methodology for designing maximum allowable wellhead pressure for CO_2 injection: application to the Shenhua CCS demonstration project, China. *Greenhouse Gases: Science and Technology*, **7**(1): 158–181. doi:10.1002/ghg.1640.

Bai M, Sun J, Song K, et al. 2015. Evaluation of mechanical well integrity during CO_2 underground storage. *Environmental Earth Sciences*, **73**: 6815–6825. doi:10.1007/s12665-015-4157-5.

Benali B, Føyen TL, Alcorn ZP, et al. 2022. Pore-scale bubble population dynamics of CO_2-foam at reservoir pressure. *International Journal of Greenhouse Gas Control*, **114**: 103607. doi:10.1016/j.ijggc.2022.103607.

Bense VF, Gleeson T, Loveless SE, et al. 2013. Fault zone hydrogeology. *Earth-Science Reviews*, **127**: 171–192. doi:10.1016/j.earscirev.2013.09.008.

Bensinger J, Beckingham LE. 2020. CO_2 storage in the Paluxy formation at the Kemper County CO_2 storage complex: Pore network properties and simulated reactive permeability evolution. *International Journal of Greenhouse Gas Control*, **93**: 102887. doi:10.1016/j.ijggc.2019.102887.

Birkholzer JT, Zhou Q, Tsang CF. 2009. Large-scale impact of CO_2 storage in deep saline aquifers: A sensitivity study on pressure response in stratified systems. *International Journal of Greenhouse Gas Control*, **3**: 181–194. doi:10.1016/j.ijggc.2008.08.002.

Blunt MJ, Bijeljic B, Dong H, et al. 2013. Pore-scale imaging and modelling. *Advances in Water Resources*, **51**: 197–217. doi:10.1016/j.advwatres.2012.03.003.

Brantley SL, Conrad CF. 2008. Analysis of rates of geochemical reactions. In: *Kinetics of Water-Rock Interaction*, Springer, pp. 1–37. doi:10.1007/978-0-387-73563-4 1.

Bryant SL, Lakshminarasimhan S, Pope GA. 2008. Buoyancy-dominated multiphase flow and its effect on geological sequestration of CO_2. *SPE Journal*, **13**(04): 447–454. doi:10.2118/99938-PA.

Caine JS, Evans JP, Forster CB. 1996. Fault zone architecture and permeability structure. *Geology*, **24**(11): 1025–1028. doi:10.1130/0091-7613(1996)024<1025:FZAAPS>2.3.CO;2.

Calabrese M, Masserano F, Blunt MJ. 2005. Simulation of physical–chemical processes during carbon dioxide sequestration in geological structures. *SPE Annual Technical Conference and Exhibition*, SPE 95820-MS. doi:10.2118/95820-MS.

Campos R, Barrios I, Lillo J. 2015. Experimental CO_2 injection: Study of physical changes in sandstone porous media using Hg porosimetry and 3D pore network models. *Energy Reports*, **1**: 71–79. doi:10.1016/j.egyr.2015.01.004.

Cappa F, Rutqvist J. 2011. Modeling of coupled deformation and permeability evolution during fault reactivation induced by deep underground injection of CO_2. *International Journal of Greenhouse Gas Control*, **5**: 336–346. doi:10.1016/j.ijggc.2010.08.005.

Carrillo FJ, Bourg IC. 2021. Capillary and viscous fracturing during drainage in porous media. *Physical Review E*, **103**(6): 063106. doi:10.1103/PhysRevE.103.063106.

Carroll S, Carey JW, Dzombak D, et al. 2016. Role of chemistry, mechanics, and transport on well integrity in CO_2 storage environments. *International Journal of Greenhouse Gas Control*, **49**: 149–160. doi:10.1016/j.ijggc.2016.01.010.

Celia MA, Bachu S, Nordbotten JM, et al. 2015. Status of CO_2 storage in deep saline aquifers with emphasis on modeling approaches and practical simulations. *Water Resources Research*, **51**(9): 6846–6892. doi:10.1002/2015WR017609.

Celia MA, Bachu S, Nordbotten JM, et al. 2005. Quantitative estimation of CO_2 leakage from geological storage: Analytical models, numerical models and data needs. it Greenhouse Gas Control Technologies 7, **I**:663–671. doi:10.1016/B978-008044704-9/50067-7.

Chadwick RA, Arts R, Bentham M, et al. 2009. Review of Monitoring Issues and Technologies Associated with the Long-Term Underground Storage of Carbon Dioxide. *Geological Society, London, Special Publications*, **313**: 257–275. doi:10.1144/SP313.15.

Chaturvedi KR, Ravilla D, Kaleem W, et al. 2021. Impact of low salinity water injection on CO_2 storage and oil recovery for improved CO_2 utilization. *Chemical Engineering Science*, **229**: 116127. doi:10.1016/j.ces.2020.116127.

Chen B, Barboza BR, Sun Y, et al. 2021. A review of hydraulic fracturing simulation. *Archives of Computational Methods in Engineering*, **28**: 3185–3242. doi:10.1007/s11831-021-09653-z.

Chen B, Li Q, Tan Y, et al. 2024. Experimental measurements and characterization models of caprock breakthrough pressure for CO_2 geological storage. *Earth-Science Reviews*, **252**: 104732. doi:10.1016/j.earscirev.2024.104732.

Chester FM, Logan JM. 1986. Implications for mechanical properties of brittle faults from observations of the Punchbowl fault zone, California. *Pure and Applied Geophysics*, **124**: 80–106. doi:10.1007/BF00875720.

Childs C, Manzocchi T, Walsh JJ, et al. 2009. A geometric model of fault zone and fault rock thickness variations. *Journal of Structural Geology*, **31**: 117–127. doi:10.1016/j.jsg.2008.08.009.

Cho J, Kim TH, Chang N, et al. 2019. Effects of asphaltene deposition-derived formation damage on three-phase hysteretic models for prediction of coupled CO_2 enhanced oil recovery and storage performance. *Journal of Petroleum Science and Engineering*, **172**: 988–997. doi:10.1016/j.petrol.2018.09.006.

Cui G, Hu Z, Wang Y, et al. 2024. Migration characteristics and local capillary trap mechanism after the CO_2 leakage out of saline aquifers. *Fuel*, **356**: 129347. doi:10.1016/j.fuel.2023.129347.

Dai Z, Zhan C, Dong S, et al. 2020. How does resolution of sedimentary architecture data affect plume dispersion in multiscale and hierarchical systems? *Journal of Hydrology*, **582**: 124516. doi:10.1016/j.jhydrol.2019.124516.

Dashtian H, Bakhshian S, Hajirezaie S, et al. 2019. Convection-diffusion-reaction of CO_2-enriched brine in porous media: a pore-scale study. *Computers & Geosciences*, **125**: 19–29. doi:10.1016/j.cageo.2019.01.009.

Davoodi S, Al-Shargabi M, Wood DA, et al. 2024. Carbon dioxide sequestration through enhanced oil recovery: A review of storage mechanisms and technological applications. *Fuel*, **366**: 131313. doi:10.1016/j.fuel.2024.131313.

De Silva GPD, Ranjith PG, Perera MSA. 2015. Geochemical aspects of CO_2 sequestration in deep saline aquifers: a review. *Fuel*, **155**: 128–143. doi:10.1016/j.fuel.2015.03.045.

Ding Y, Li S, Zhu B, et al. 2023. Research on the feasibility of storage and estimation model of storage capacity of CO_2 in fissures of coal mine old goaf. *International Journal of Mining Science and Technology*, **33**(6): 675–686. doi:10.1016/j.ijmst.2023.03.003.

Dooley JJ, Dahowski RT, Davidson CL, et al. 2006. Carbon Dioxide Capture and Geologic Storage: A Core Element of a Global Energy Technology Strategy. *Pacific Northwest National Laboratory Report*, PNNL-15106. doi:10.2172/882024.

Doughty C, Pruess K, Benson SM, et al. 2001. Capacity investigation of brine-bearing sands of the Frio Formation for geologic sequestration of CO_2. *Proceedings of the First National Conference on Carbon Sequestration*, Washington, D.C., May 14–17, 2001. U.S. Department of Energy, National Energy Technology Laboratory, CD-ROM USDOE/NETL-2001/1144, Paper P.32.

Ducellier A, Seyedi D, Foerster E. 2011. A coupled hydromechanical fault model for the study of the integrity and safety of geological storage of CO_2. *Energy Procedia*, **4**: 5138–5145. doi:10.1016/j.egypro.2011.02.490.

Egermann P, Bazin B, Vizika O. 2005. An experimental investigation of reaction-transport phenomena during CO_2 injection. *SPE Annual Technical Conference and Exhibition*, SPE 93674, Bahrain, March 2005. doi:10.2118/93674-MS.

Ellis JS, Bazylak A. 2012. Dynamic pore network model of surface heterogeneity in brine-filled porous media for carbon sequestration. *Physical Chemistry Chemical Physics*, **14**(23): 8382–8390. doi:10.1039/c2cp40812k.

Ennis-King J, Paterson L. 2002. Engineering aspects of geological sequestration of carbon dioxide. *SPE Asia Pacific Oil and Gas Conference and Exhibition*, SPE 77809, Melbourne, Australia, October 8–10, 2002. doi:10.2118/77809-MS.

Evans J. 2013. Analysis of Potential Leakage Pathways and Mineralization within Caprocks for Geologic Storage of CO_2. Distributed by the Office of Scientific and Technical Information, U.S. Dept. of Energy, Utah State University.

Fakhari A, Li Y, Bolster D, et al. 2018. A phase-field lattice Boltzmann model for simulating multiphase flows in porous media: Application and comparison to experiments of CO_2 sequestration at pore scale. *Advances in Water Resources*, **114**: 119–134. doi:10.1016/j.advwatres.2018.02.005.

Fan Z, Xu T, Yang B, et al. 2023. Numerical simulation of thermo-hydro-mechanical-chemical response caused by CO_2 injection into saline geological formations: a case study from the Ordos project, China. *Acta Geologica Sinica (English Edition)*, **97**: 889–910. doi:10.1111/1755-6724.15084.

Faulkner D. 2004. A model for the variation in permeability of clay-bearing fault gouge with depth in the brittle crust. *Geophysical Research Letters*, **31**: L19611. doi:10.1029/2004GL020736.

Faulkner D, Jackson C, Lunn R, et al. 2010. A review of recent developments concerning the structure, mechanics and fluid flow properties of fault zones. *Journal of Structural Geology*, **32**: 1557–1575. doi:10.1016/j.jsg.2010.06.009.

Fernø MA, Haugen M, Eikehaug K, et al. 2024. Room-scale CO_2 injections in a physical reservoir model with faults. *Transport in Porous Media*, **151**: 913–937. doi:10.1007/s11242-023-02013-4.

Ferrari A, Lunati I. 2013. Direct numerical simulations of interface dynamics to link capillary pressure and total surface energy. *Advances in Water Resources*, **57**: 19–31. doi:10.1016/j.advwatres.2013.03.005.

Flett MA, Gurton RM, Taggart IJ. 2005. Heterogeneous saline formations: Long-term benefits for geo-sequestration of greenhouse gases. *Proceedings of the 7th International Conference on Greenhouse Gas Control Technologies (GHGT-7)*, Vancouver, Canada, September 5–9, 2004, Vol. I, pp. 501–510. doi:10.1016/B978-008044704-9/50051-3

Gan Q, Candela T, Wassing B, et al. 2021. The use of supercritical CO_2 in deep geothermal reservoirs as a working fluid: Insights from coupled THMC modeling. *International Journal of Rock Mechanics and Mining Sciences*, **147**: 104872. doi:10.1016/j.ijrmms.2021.104872.

Gaus I, Azaroual M, Czernichowski-Lauriol I. 2005. Reactive transport modelling of the impact of CO_2 injection on the clayey cap rock at Sleipner (North Sea). *Chemical Geology*, **217**: 319–337. doi:10.1016/j.chemgeo.2004.12.016.

Gaus I. 2010. Role and impact of CO_2–rock interactions during CO_2 storage in sedimentary rocks. *International Journal of Greenhouse Gas Control*, **4**: 73–89. doi:10.1016/j.ijggc.2009.09.015.

Ge J, Zhang X, Le-Hussain FF. 2022. Fines migration and mineral reactions as a mechanism for CO_2 residual trap during CO_2 sequestration. *Energy*, **239**: 122233. doi:10.1016/j.energy.2021.122233.

Geloni C, Giorgis T, Battistelli A. 2011. Modeling of rocks and cement alteration due to CO_2 injection in an exploited gas reservoir. *Transport in Porous Media*, **90**: 183–200. doi:10.1007/s11242-011-9714-0.

Gholami R, Raza A, Iglauer S. 2021. Leakage risk assessment of a CO_2 storage site: a review. *Earth-Science Reviews*, **223**: 103849. doi:10.1016/j.earscirev.2021.103849.

Gray KE, Podnos E, Becker E. 2009. Finite-element studies of near-wellbore region during cementing operations: Part I. *SPE Drilling & Completion*, **24**: 127–136. doi:10.2118/106998-MS.

Griffith CA, Dzombak DA, Lowry GV. 2011. Physical and chemical characteristics of potential seal strata in regions considered for demonstrating geological saline CO_2 sequestration. *Environmental Earth Sciences*, **64**: 925–948. doi:10.1007/s12665-011-0911-5.

Guglielmi Y, Birkholzer J, Rutqvist J, et al. 2017. Can fault leakage occur before or without reactivation? Results from an in-situ fault reactivation experiment at Mont Terri. *Energy Procedia*, **114**: 3167–3174. doi:10.1016/j.egypro.2017.03.1445.

Guglielmi Y, Nussbaum C, Cappa F, et al. 2021. Aseismic leakage in caprock analogs: implications for CO_2 sequestration. *International Journal of Greenhouse Gas Control*, **111**: 103471. doi:10.1016/j.ijggc.2021.103471.

Gundogar AS, Ross CM, Akin S, et al. 2016. Multiscale pore structure characterization of Middle East carbonates. *Journal of Petroleum Science and Engineering*, **146**: 570–583. doi:10.1016/j.petrol.2016.07.018.

Gunter WD, Perkins E, McCann TJ. 1993. Aquifer disposal of CO_2-rich gases: reaction design for added capacity. *Energy Conversion and Management*, **34**: 941–948. doi:10.1016/0196-8904(93)90040-H.

Guo R, Dalton LE, Fan M, et al. 2020. The role of the spatial heterogeneity and correlation length of surface wettability on two-phase flow in a CO_2-water-rock system. *Advances in Water Resources*, **146**: 103763. doi:10.1016/j.advwatres.2020.103763.

Gysi AP, Stefánsson A. 2012. CO_2-water-basalt interaction: Low temperature experiments and implications for CO_2 sequestration into basalts. *Geochimica et Cosmochimica Acta*, **81**: 129–152. doi:10.1016/j.gca.2011.12.012.

Hu R, Wan J, Kim Y, et al. 2017. Wettability effects on supercritical CO_2–brine immiscible displacement during drainage: Pore-scale observation and 3D simulation. *International Journal of Greenhouse Gas Control*, **60**: 129–139. doi:10.1016/j.ijggc.2017.03.011.

Huber EJ, Stroock AD, Koch DL. 2016. Analysis of a time dependent injection strategy to accelerate the residual trapping of sequestered CO_2 in the geologic subsurface. *International Journal of Greenhouse Gas Control*, **44**: 185–198. doi:10.1016/j.ijggc.2015.11.024.

Islam M, Huerta N, Dilmore R. 2020. Effect of computational schemes on coupled flow and geo-mechanical modeling of

CO_2 leakage through a compromised well. *Computation*, **8**(4): 98. doi:10.3390/computation8040098.

Jackson SJ, Gunning J, Ennis-King J, et al. 2024. Tracking a subsurface CO_2 plume with time-lapse pressure tomography in the Otway Stage 3 field project. *International Journal of Greenhouse Gas Control*, **133**: 104099. doi:10.1016/j.ijggc.2024.104099.

Javadpour F, Nicot JP. 2011. Enhanced CO_2 storage and sequestration in deep saline aquifers by nanoparticles: Commingled disposal of depleted uranium and CO_2. *Transport in Porous Media*, **89**: 265–284. doi:10.1007/s11242-011-9768-z.

Jayasekara DW, Ranjith PG, Wanniarachchi WAM, et al. 2020. Effect of salinity on supercritical CO_2 permeability of caprock in deep saline aquifers: an experimental study. *Energy*, **191**: 116486. doi:10.1016/j.energy.2019.116486.

Jiang F, Tsuji T. 2016. Numerical investigations on the effect of initial state CO_2 topology on capillary trapping efficiency. *International Journal of Greenhouse Gas Control*, **49**: 179–191. doi:10.1016/j.ijggc.2016.03.006.

Jin L, Hawthorne S, Sorensen J, et al. 2017. Advancing CO_2 enhanced oil recovery and storage in unconventional oil play—Experimental studies on Bakken shales. *Applied Energy*, **208**: 171–183. doi:10.1016/j.apenergy.2017.10.054.

Johnson JW, Nitao JJ, Morris JP. 2005. Reactive transport modeling of cap-rock integrity during natural and engineered CO_2 storage. In: *Carbon Dioxide Capture for Storage in Deep Geologic Formations*, S. M. Benson (ed.), Elsevier, pp. 579–612. doi:10.1016/B978-008044570-0/50134-3.

Kanakiya S, Adam L, Esteban L, et al. 2017. Dissolution and secondary mineral precipitation in basalts due to reactions with carbonic acid. *Journal of Geophysical Research: Solid Earth*, **122**: 4312–4327. doi:10.1002/2017JB014019.

Kang YL, Xu CY, You LJ, et al. 2015. Comprehensive prediction of dynamic fracture width for formation damage control in fractured tight gas reservoir. *International Journal of Oil, Gas and Coal Technology*, **9**(3): 296–310. doi:10.1504/IJOGCT.2015.069014.

Karimnezhad M, Jalalifar H, Kamari M. 2014. Investigation of caprock integrity for CO_2 sequestration in an oil reservoir using a numerical method. *Journal of Natural Gas Science and Engineering*, **21**: 1127–1137. doi:10.1016/j.jngse.2014.10.031.

Khan MJ, Mahmood SM, Alakbari FS, et al. 2024. Rock wettability and its implication for caprock integrity in CO_2–brine systems: a comprehensive review. *Energy & Fuels*, **38**: 19966–19991. doi:10.1021/acs.energyfuels.4c02736.

Klotz D, Seiler KP, Moser H, et al. 1980. Dispersivity and velocity relationship from laboratory and field experiments. *Journal of Hydrology*, **47**: 135–150. doi:10.1016/0022-1694(80)90018-9.

Krevor S, Pini R, Li B, et al. 2011. Capillary heterogeneity trapping of CO_2 in a sandstone rock at reservoir conditions. *Geophysical Research Letters*, **38**(15): L15402. doi:10.1029/2011GL048239.

Krishnamurthy PG, DiCarlo D, Meckel T. 2022. Geologic heterogeneity controls on trapping and migration of CO_2. *Geophysical Research Letters*, **49**(16): e2022GL099104. doi:10.1029/2022GL099104.

Lasaga AC, Soler JM, Ganor J, et al. 1994. Chemical weathering rate laws and global geochemical cycles. *Geochimica et Cosmochimica Acta*, **58**: 2361–2386. doi:10.1016/0016-7037(94)90016-7.

Lecampion B, Bunger A, Zhang X. 2018. Numerical methods for hydraulic fracture propagation: A review of recent trends. *Journal of Natural Gas Science and Engineering*, **49**: 66–83. doi:10.1016/j.jngse.2017.10.012.

Lee S-Y, Mohamed FR, Lee KH, et al. 2023. Probabilistic evaluation of geomechanical risks in CO_2 storage: an exploration of caprock integrity metrics using a multilaminate model. *Energies*, **16**: 6954. doi:10.3390/en16196954.

Li Q, Wu Z, Bai Y, et al. 2006. Thermo-hydro-mechanical modeling of CO_2 sequestration system around fault environment. *Pure and Applied Geophysics*, **163**: 2585–2593. doi:10.1007/s00024-006-0141-z.

Li WP, Cao DP, Qiao W, et al. 2025. Key technologies for exploration and geological evaluation of deep carbon storage spaces. *Journal of China Coal Society*, **50**(5): 2333–2354. doi:10.13225/j.cnki.jccs.2025.0527.

Li X, Li Q, Bai B, et al. 2016. The geomechanics of Shenhua carbon dioxide capture and storage (CCS) demonstration project in Ordos Basin, China. *Journal of Rock Mechanics and Geotechnical Engineering*, **8**: 948–966. doi:10.1016/j.jrmge.2016.07.002.

Li XR, Gu CW, Ding ZC, et al. 2023. THM coupled analysis of cement sheath integrity considering well loading history. *Petroleum Science*, **20**: 447–459. doi:10.1016/j.petrol.2022.11.027.

Limousin G, Gaudet JP, Charlet L, et al. 2007. Sorption isotherms: A review on physical bases, modeling and measurement. *Applied Geochemistry*, **22**: 249–275. doi:10.1016/j.apgeochem.2006.09.010.

Lindeberg E, Wessel-Berg D. 1997. Vertical convection in an aquifer column under a gas cap of CO_2. *Energy Conversion and Management*, **38**(Suppl.): S229–S234. doi:10.1016/S0196-8904(96)00274-9.

Lippmann MJ, Benson SM. 2003. Relevance of underground natural gas storage to geologic sequestration of carbon dioxide. U.S. Department of Energy, Office of Scientific and Technical Information, Report No. OSTI ID 813565.

Liu B, Suzuki A, Ito T. 2020. Estimating the seepage effect of SC-CO_2 and water fracturing with a steady-state flow model considering capillary and viscous forces at the pore scale. *Journal of Petroleum Science and Engineering*, **184**: 106483. doi:10.1016/j.petrol.2019.106483.

Liu H, Valocchi AJ, Werth C, et al. 2014. Pore-scale simulation of liquid CO_2 displacement of water using a two-phase lattice Boltzmann model. *Advances in Water Resources*, **73**: 144–158. doi:10.1016/j.advwatres.2014.07.012.

Liu F, Lu P, Zhu C, et al. 2011. Coupled reactive flow and transport modeling of CO_2 sequestration in the Mt. Simon sandstone formation, Midwest U.S.A. *International Journal of Greenhouse Gas Control*, **5**: 294–307. doi:10.1016/j.ijggc.2010.11.001.

Liu HH, Bodvarsson GS, Zhang G. 2004. Scale dependency of the effective matrix diffusion coefficient. *Vadose Zone Journal*, **3**: 312–320. doi:10.2136/vzj2004.3120.

Liu T, Li Q, Li X, et al. 2024. A critical review of distributed fiber optic sensing applied to geologic carbon dioxide storage. *Gases: Science and Technology*, **14**: 676–694. doi:10.3390/gases14040048.

Luo HM, Li JY, Xie CJ, et al. 2025. Sealing performance of compressed air energy storage spaces in aquifers: key issues and progress. *Petroleum Geology and Recovery Efficiency*, **32**(5): 19–34. doi:10.13673/j.pgre.202404009

Ma B, Cao Y, Zhang Y, et al. 2020. Role of CO_2-water-rock interactions and implications for CO_2 sequestration in Eocene deeply buried sandstones in the Bonan Sag, eastern Bohai Bay Basin, China. *Chemical Geology*, **541**: 119585. doi:10.1016/j.chemgeo.2020.119585.

Martinez MJ, Newell P, Bishop JE, et al. 2013. Coupled multiphase flow and geomechanics model for analysis of joint reactivation during CO_2 sequestration operations. *International Journal of Greenhouse Gas Control*, **17**: 148–160. doi:10.1016/j.ijggc.2013.05.004.

Meng FK, Ren L, Su Y L, et al. 2014. Displacement characteristic of CO_2 flooding in low permeability reservoirs based on pore scale. *Journal of Xi'an Shiyou University (Natural Science Edition)*, **29**(5): 61–65+7.

Michael K, Avijegon A, Ricard L, et al. 2021. A (not so) shallow controlled CO_2 release experiment in a fault zone. *Proceedings of the 15th Greenhouse Gas Control Technologies Conference (GHGT-15)*, Amsterdam, Netherlands, March 15–18, 2021.

Middleton RS, Keating GN, Stauffer PH, et al. 2012. The cross-scale science of CO_2 capture and storage: from pore scale to regional scale. *Energy & Environmental Science*, **5**(6): 7328–7345. doi:10.1039/C2EE03425E.

Mishra A, Haese RR. 2020. Quantification of the turning point saturation for cross bedded CO_2 storage reservoirs. *International Journal of Greenhouse Gas Control*, **103**: 103185. doi:10.1016/j.ijggc.2020.103185.

Mitiku AB, Li D, Bauer S, et al. 2013. Geochemical modelling of CO_2-water-rock interactions in a potential storage formation of the North German sedimentary basin. *Applied Geochemistry*, **36**: 168–186. doi:10.1016/j.apgeochem.2013.05.007.

Mohammed Sajed OK, Glover PWJ. 2020. Dolomitisation, cementation and reservoir quality in three Jurassic and Cretaceous carbonate reservoirs in North-Western Iraq. *Marine and Petroleum Geology*, **115**: 104256. doi:10.1016/j.marpetgeo.2020.104256.

Molins S, Trebotich D, Yang L, et al. 2014. Pore-scale controls on calcite dissolution rates from flow-through laboratory and numerical experiments. *Environmental Science & Technology*, **48**: 7453–7460. doi:10.1021/es500924n.

Morris JP, Hao Y, Foxall W, et al. 2011. A study of injection-induced mechanical deformation at the In Salah CO_2 storage project. *International Journal of Greenhouse Gas Control*, **5**: 270–280. doi:10.1016/j.ijggc.2010.10.004.

Nath F, Cabezudo E, Romero NG. 2024. Experimental investigations of caprock integrity for geological carbon storage using three-dimensional digital image correlation. *SPE Western Regional Meeting*, SPE D031S014R002, 2024. doi:10.2118/218920-MS

Nguyen C, Loi G, Russell T, et al. 2024. Physics mechanisms of fines detachment and migration during CO_2-water corefloods. *arXiv preprint*, arXiv:2403.14343. https://arxiv.org/pdf/2403.14343

Noiriel C, Daval D. 2017. Pore-scale geochemical reactivity associated with CO_2 storage: new frontiers at the fluid-solid interface. *Accounts of Chemical Research*, **50**: 759–768. doi:10.1021/acs.accounts.7b00019.

Nordbotten JM, Celia MA, Bachu S. 2005. Injection and storage of CO_2 in deep saline aquifers: analytical solution for CO_2 plume evolution during injection. *Transport in Porous Media*, **58**: 339–360. doi:10.1007/s11242-004-0670-9.

Nygaard R, Salehi S, Weideman B, et al. 2014. Effect of dynamic loading on wellbore leakage for the Wabamun area CO_2-sequestration project. *Journal of Canadian Petroleum Technology*, **53**: 69–82. doi:10.2118/146640-PA.

Olivella S, Carrera J, Gens A, Alonso E E. 1994. Non-isothermal multiphase flow of brine and gas through saline media. *Transport in Porous Media*, **15**: 271–293. doi:10.1007/BF00613282.

Orlic B, ter Heege J, Wassing B. 2011. Assessing the integrity of fault- and top seals at CO_2 storage sites. *Energy Procedia*, **4**: 4798–4805. doi:10.1016/j.egypro.2011.02.445.

Orr FM. 2009. Onshore geologic storage of CO_2. *Science*, **325**(5948): 1656–1658. doi:10.1126/science.1175677.

Palandri JL, Kharaka YK. 2005. Ferric iron-bearing sediments as a mineral trap for CO_2 sequestration: Iron reduction using sulfur-bearing waste gas. *Chemical Geology*, **217**: 351–364. doi:10.1016/j.chemgeo.2004.12.018.

Pan PZ, Rutqvist J, Feng -T, et al. 2013. Modeling of caprock discontinuous fracturing during CO_2 injection into a deep brine aquifer. *International Journal of Greenhouse Gas Control*, **19**: 559–575. doi:10.1016/j.ijggc.2013.10.016.

Pan X, Sun L, Liu Q, et al. 2025. Mechanism of CO_2 flooding in shale reservoirs–insights from nanofluids. *Nanoscale*, **17**(3): 1524–1535. doi:10.1039/D4NR02474E.

Peacock DCP, Mann A. 2005. Evaluation of the controls on fracturing in reservoir rocks. *Journal of Petroleum Geology*, **28**(4): 385–396. doi:10.1111/j.1747-5457.2005.tb00089.x.

Rashid F, Glover PWJ, Lorinczi P, et al. 2015. Porosity and permeability of tight carbonate reservoir rocks in the north of Iraq. *Journal of Petroleum Science and Engineering*, **133**: 147–161. doi:10.1016/j.petrol.2015.05.009.

Rathnaweera TD, Ranjith PG. 2020. Nano-modified CO_2 for enhanced deep saline CO_2 sequestration: a review and perspective study. *Earth-Science Reviews*, **200**: 103035. doi:10.1016/j.earscirev.2019.103035.

Raza A, Glatz G, Gholami R, et al. 2022. Carbon mineralization and geological storage of CO_2 in basalt: Mechanisms and technical challenges. *Earth-Science Reviews*, **229**: 104036. doi:10.1016/j.earscirev.2022.104036.

Raza A, Rezaee R, Gholami R, et al. 2016. A screening criterion for selection of suitable CO_2 storage sites. *Journal of Natural Gas Science and Engineering*, **28**: 317–327. doi:10.1016/j.jngse.2015.11.053.

Raziperchikolaee S, Pasumarti A. 2020. The impact of the depth-dependence of in-situ stresses on the effectiveness of stacked caprock reservoir systems for CO_2 storage. *Journal of Natural Gas Science and Engineering*, **79**: 103361. doi:10.1016/j.jngse.2020.103361.

Raziperchikolaee S, Alvarado V, Yin S. 2013. Effect of hydraulic fracturing on long-term storage of CO_2 in stimulated saline aquifers. *Applied Energy*, **102**: 1091–1104. doi:10.1016/j.apenergy.2012.06.043.

Raziperchikolaee S, Kelley M, Gupta N. 2019. A screening framework study to evaluate CO_2 storage performance in single and stacked caprock–reservoir systems of the Northern Appalachian Basin. *Greenhouse Gases: Science and Technology*, **9**: 582–605. doi:10.1002/ghg.1873.

Reimus PW, Callahan TJ. 2007. Matrix diffusion rates in fractured volcanic rocks at the Nevada Test Site: Evidence for a dominant influence of effective fracture apertures. *Water Resources Research*, **43**: W05425. doi:10.1029/2006WR005746.

Reinicke KM, Fichter C. 2010. Measurement strategies to evaluate the integrity of deep wells for CO_2 applications. In: *Underground Storage of CO_2 and Energy*, Springer, pp. 67–89.

Ren B, Sun Y, Bryant S. 2014. Maximizing local capillary trapping during CO_2 injection. *Energy Procedia*, **63**: 5562–5576. doi:10.1016/j.egypro.2014.11.590.

Rutqvist J, Tsang CF. 2002. A study of caprock hydromechanical changes associated with CO_2-injection into a brine formation. *Environmental Geology*, **42**: 296–305. doi:10.1007/s00254-001-0499-2.

Rutqvist J. 2012. The geomechanics of CO_2 storage in deep sedimentary formations. *Geotechnical and Geological Engineering*, **30**: 525–551. doi:10.1007/s10706-011-9491-0.

Rutqvist J, Birkholzer J, Cappa F, et al. 2007. Estimating maximum sustainable injection pressure during geological sequestration of CO_2 using coupled fluid flow and geomechanical fault-slip analysis. *Energy Conversion and Management*, **48**(6): 1798–1807. doi:10.1016/j.enconman.2007.01.021.

Rutqvist J, Birkholzer JT, et al. 2008. Coupled reservoir–geomechanical analysis of the potential for tensile and shear failure associated with CO_2 injection in multilayered reservoir–caprock systems. *International Journal of Rock Mechanics and Mining Sciences*, **45**: 132–143. doi:10.1016/j.ijrmms.2007.04.006.

Rutqvist J, Wu YS, Tsang CF, et al. 2002. A modeling approach for analysis of coupled multiphase fluid flow, heat transfer, and deformation in fractured porous rock. *International Journal of Rock Mechanics and Mining Sciences*, **39**(4): 429–442. doi:10.1016/S1365-1609(02)00022-9.

Davis SJ, Lewis NS, Shaner M, et al. 2018. Net-zero emissions energy systems. *Science*, **360**(6393): eaas9793. doi:10.1126/science.aas9793.

Saadatpoor E, Bryant SL, Sepehrnoori K. 2009. New trapping mechanism in carbon sequestration. *Transport in Porous Media*, **82**(1): 3–17. doi:10.1007/s11242-009-9446-6.

Sbai MA, Azaroual M. 2011. Numerical modeling of formation damage by two-phase particulate transport processes during CO_2 injection in deep heterogeneous porous media. *Advances in Water Resources*, **34**(1): 62–82. doi:10.1016/j.advwatres.2010.09.009.

Shan X, Chen H. 1993. Lattice Boltzmann model for simulating flows with multiple phases and components. *Physical Review E*, **47**(3): 1815–1819. doi:10.1103/PhysRevE.47.1815.

Shen N, Li X, Zhang Q, et al. 2021. Comparison of shear-induced gas transmissivity of tensile fractures in sandstone and shale under varying effective normal stresses. *Journal of Natural Gas Science and Engineering*, **95**: 104218. doi:10.1016/j.jngse.2021.104218.

Shi J, Xue Z, Durucan S. 2010. Supercritical CO_2 core flooding and imbibition in Tako sandstone—Influence of sub-core scale heterogeneity. *International Journal of Greenhouse Gas Control*, **5**(1): 75–87. doi:10.1016/j.ijggc.2010.07.003.

Shukla R, Ranjith P, Haque A, et al. 2010. A review of studies on CO_2 sequestration and caprock integrity. *Fuel*, **89**: 2651–2664. doi:10.1016/j.fuel.2010.05.012.

Snæbjörnsdóttir S, Sigfússon B, Marieni C, et al. 2020. Carbon dioxide storage through mineral carbonation. *Nature Reviews Earth & Environment*, **1**: 90–102. doi:10.1038/s43017-019-0011-8.

Song J, Zhang D. 2013. Comprehensive review of caprock-sealing mechanisms for geologic carbon sequestration. *Environmental Science & Technology*, **47**: 9–22. doi:10.1021/es301610p.

Sun G, Sun Z, Fager A, et al. 2023. Pore-scale analysis of CO_2-brine displacement in Berea sandstone and its implications to CO_2 injectivity. *E3S Web of Conferences*, **414**: 1011. doi:10.1051/e3sconf/202336701011.

Sun Z, Salazar-Tio R, Wu L, et al. 2023. Geomechanical assessment of a large-scale CO_2 storage and insights from uncertainty analysis. *Geoenergy Science and Engineering*, **224**: 211596. doi:10.1016/j.geoen.2023.211596.

Sun Z, Sun G, Salazar-Tio R, et al. 2025. A comprehensive review of CO_2 geological storage projects with regulatory requirements of computational modeling. *Fuel*, **386**: 134209. doi:10.1016/j.fuel.2024.134209.

Tan Q, Peng H, Tian J, et al. 2025. A review on mechanisms of CO_2-fluid-rock interaction during CO_2 injection into carbonate reservoirs. *Geoenergy Science and Engineering*, **249**: 213773. doi:10.1016/j.geoen.2025.213773.

Thompson N, Andrews JS, Bjørnarå TI. 2021. Assessing potential thermo-mechanical impacts on caprock due to CO_2 injection—a case study from northern lights CCS. *Energies*, **14**: 5054. doi:10.3390/en14165054.

Vialle S, Druhan JL, Maher K. 2016. Multi-phase flow simulation of CO_2 leakage through a fractured caprock in response to mitigation strategies. *International Journal of Greenhouse Gas Control*, **44**: 11–25. doi:10.1016/j.ijggc.2015.10.007.

Vilarrasa V, Bolster D, Olivella S, et al. 2010. Coupled hydromechanical modeling of CO_2 sequestration in deep saline aquifers. *International Journal of Greenhouse Gas Control*, **4**(6): 910–919. doi:10.1016/j.ijggc.2010.06.006.

Vilarrasa V, Olivella S, Carrera J. 2011. Geomechanical stability of the caprock during CO_2 sequestration in deep saline aquifers. *Energy Procedia*, **4**: 5306–5313. doi:10.1016/j.egypro.2011.02.511.

Wang W, Liang Z, Zuo J, et al. 2025. The pore structure changes and CO_2 migration dynamic characteristics in tight sandstone during supercritical CO_2 geosequestration: A case study in the Chang 7 layer, Ordos Basin, China. *Fuel*, **379**: 133019. doi:10.1016/j.fuel.2024.133019.

White SP, Allis RG, Moore J, et al. 2005. Simulation of reactive transport of injected CO_2 on the Colorado Plateau, Utah, USA. *Chemical Geology*, **217**: 291–309. doi:10.1016/j.chemgeo.2004.12.020.

White AF, Blum AE, Schulz MS, et al. 1996. Chemical weathering of a soil chronosequence on granite alluvium I. Reaction rates based on changes in soil mineralogy. *Geochimica et Cosmochimica Acta*, **60**: 2533–2550. doi:10.1016/0016-7037(96)00106-8.

Wigand M, Kaszuba JP, Carey JW, et al. 2009. Geochemical effects of CO_2 sequestration on fractured wellbore cement at the cement/caprock interface. *Chemical Geology*, **265**: 122–133. doi:10.1016/j.chemgeo.2009.04.008.

Wu H, Bai B, Li X. 2018. An advanced analytical solution for pressure build-up during CO_2 injection into infinite saline aquifers: The role of compressibility. *Advances in Water Resources*, **112**: 95–105. doi:10.1016/j.advwatres.2017.12.010.

Wu HQ, Bai B, Li X, et al. 2016. An explicit integral solution for pressure build-up during CO_2 injection into infinite saline aquifers. *Greenhouse Gases: Science and Technology*, **6**(5): 633–647. doi:10.1002/ghg.1601.

Wu H, Vilarrasa V, De Simone S, et al. 2021. Analytical solution to assess the induced seismicity potential of faults in pressurized and depleted reservoirs. *Journal of Geophysical Research: Solid Earth*, **126**(1): e2020JB020436. doi:10.1029/2020JB020436.

Xiao T, Xu H, Moodie N, et al. 2020. Chemical-mechanical impacts of CO_2 intrusion into heterogeneous caprock. *Water Resources Research*, **56**: e2020WR027650. doi:10.1029/2020WR027193.

Xu L, Li Q, Tan Y, et al. 2022. Characterization of carbon dioxide leakage process along faults in the laboratory. *Journal of Rock Mechanics and Geotechnical Engineering*, **14**: 674–688. doi:10.1016/j.jrmge.2021.12.019.

Yang XY, Xie JY, Ye XP, et al. 2023. Mineral particles migration and injection plugging mechanism of CO_2 geological storage in low permeability reservoirs. *Journal of China Coal Society*, **48**(7): 2827–2835. doi:10.13225/j.cnki.jccs.CN23.0180.

Yang B, Zhu L, He J, et al. 2024. A feasible strategy

for depressant-free flotation separation of siderite from magnesiohornblende using a highly selective collector. *Journal of Molecular Liquids*, **394**: 123689. doi:10.1016/j.molliq.2023.123689.

Yang XJ, Buscheck TA, Mansoor K, et al. 2019. Assessment of geophysical monitoring methods for detection of brine and CO_2 leakage in drinking water aquifers. *International Journal of Greenhouse Gas Control*, **90**: 102803. doi:10.1016/j.ijggc.2019.102803.

Sun Z, Fager A, Crouse B. 2024. Modeling of thermal-mechanical impact on wellbore integrity due to CO_2 injection. *ARMA US Rock Mechanics/Geomechanics Symposium*, ARMA D041S054R003. doi:10.56952/ARMA-2024-0498.

Zhai G, Peters E, Candela T. 2024. A new geomechanical modeling workflow for CCUS near-well integrity assessment in layered poroelastic medium. *ARMA US Rock Mechanics/Geomechanics Symposium*, ARMA D042S057R019.

Zhang J. 2013. Borehole stability analysis accounting for anisotropies in drilling to weak bedding planes. *International Journal of Rock Mechanics and Mining Sciences*, **60**: 160–170. doi:10.1016/j.ijrmms.2012.12.025.

Zhang Y, Langhi L, Schaubs PM, et al. 2015. Geomechanical stability of CO_2 containment at the South West Hub Western Australia: A coupled geomechanical–fluid flow modelling approach. *International Journal of Greenhouse Gas Control*, **37**: 12–23. doi:10.1016/j.ijggc.2015.03.003.

Zhang Z, Agarwal RK. 2012. Numerical simulation and optimization of CO_2 sequestration in saline aquifers for vertical and horizontal well injection. *Computational Geosciences*, **16**: 891–899. doi:10.1016/j.compfluid.2012.04.027.

Zhang C, Oostrom M, Grate JW, et al. 2011. Liquid CO_2 displacement of water in a dual-permeability pore network micromodel. *Environmental Science & Technology*, **45**(17): 7581–7588. doi:10.1021/es201858r.

Zhang L, Yang Q, Zhang S, et al. 2024. Enhanced CO_2 storage efficiency due to the impact of faults on CO_2 migration in an interbedded saline aquifer. *International Journal of Greenhouse Gas Control*, **133**: 104104. doi:10.1016/j.ijggc.2024.104104.

Zhang Q, Geiger S, Storms JE, et al. 2025. Capillary pinning in sedimentary rocks for CO_2 storage: Mechanisms, terminology and State-of-the-Art. *International Journal of Greenhouse Gas Control*, **144**: 104385. doi:10.1016/j.ijggc.2025.104385.

Zhang Q, Li X, Bai B, et al. 2019. The shear behavior of sandstone joints under different fluid and temperature conditions. *Engineering Geology*, **257**: 105143. doi:10.1016/j.enggeo.2019.05.020.

Zhang T, Zhang W, Yang R, et al. 2021. CO_2 capture and storage monitoring based on remote sensing techniques: a review. *Journal of Cleaner Production*, **281**: 124409. doi:10.1016/j.jclepro.2020.124409.

Zhao B, MacMinn CW, Primkulov BK, et al. 2019. Comprehensive comparison of pore-scale models for multiphase flow in porous media. *Proceedings of the National Academy of Sciences of the United States of America*, **116**: 13799–13806. doi:10.1073/pnas.1901619116.

Zheng LG, Apps JA, Zhang Y, et al. 2009. On mobilization of lead and arsenic in groundwater in response to CO_2 leakage from deep geological storage. *Chemical Geology*, **268**: 281–297. doi:10.1016/j.chemgeo.2009.09.007.

Zhou YF, Hatzignatiou DG, Helland JO. 2017. On the estimation of CO_2 capillary entry pressure: implications on geological CO_2 storage. *International Journal of Greenhouse Gas Control*, **63**: 26–36. doi:10.1016/j.ijggc.2017.04.013.

Zhu W, Allison KL, Dunham EM, et al. 2020. Fault valving and pore pressure evolution in simulations of earthquake sequences and aseismic slip. *Nature Communications*, **11**: 4833. doi:10.1038/s41467-020-18598-z.